

To the Graduate Council:

I am submitting herewith a thesis written by Bhavin K Madhu entitled “Dynamic Analysis of Grid Connected Hybrid System of PV Panel and Wind Turbines for a Light Commercial Building.” I have examined the electronic copy of this thesis for form and content and recommend that it be accepted in partial fulfillment of the requirements for the degree of Master of Science, with a major in Mechanical Engineering.

---

Dr. Prakash Dhamshala  
Major advisor

We have read this thesis  
And recommend its acceptance:

---

Dr. Sagar Kapadia

---

Dr. Sumith Gunasekera

Accepted for the Council:

---

Dr. Stephanie Bellar  
Interim Dean of the Graduate School

# **Dynamic Analysis of Grid Connected Hybrid System of PV Panel and Wind Turbines for a Light Commercial Building**

A Thesis Presented for the Masters of Mechanical Engineering

The University of Tennessee at Chattanooga, Tennessee

Bhavin K Madhu

May 2010

## **DEDICATION**

I would like to dedicate this thesis to my late grandfather Vinodchandra, my grandmother Babuben, my father Kanaiyalal, my mother Jashumati, my sister Khyati for their love and inspiring me to work up to this level. Without their patience, understanding, and support, the completion of this thesis would not have been possible.

# **ACKNOWLEDGEMENT**

The satisfaction that accompanies the successful completion of this thesis would be incomplete without the mention of the people who made it possible, without whose constant guidance and encouragement would have made my efforts go in vain.

I consider it to be a privilege to express gratitude and respect towards all those who guided me through the completion of this thesis. I convey my thanks to thesis advisor Dr. Prakash Dhamshala, professor of Mechanical Engineering, The University of Tennessee at Chattanooga, USA, for providing the encouragement, constant support and guidance which was a great help to complete this thesis successfully.

I thank Dr. Sagar Kapadia and Dr. Sumith Gunasekera, for serving as committee members and giving the support, guidance and encouragement that was necessary for the completion of this thesis.

# Table of Contents

<b>DEDICATION</b>	<b>II</b>
<b>ACKNOWLEDGEMENT</b>	<b>III</b>
<b>LIST OF TABLES</b>	<b>X</b>
<b>LIST OF FIGURES</b>	<b>XI</b>
<b>CHAPTER 1 INTRODUCTION</b>	<b>1</b>
1.1 Fossil fuels	1
1.2 History of Wind Turbine	2
1.3 History of Photovoltaic	3
1.4 Hybrid System	4
<b>CHAPTER 2 PHOTOVOLTAIC ANALYSIS</b>	<b>7</b>
2.1 A Brief Glance at History of Photovoltaic	7
2.1.1 Semi Conductors	9
2.2 I-V Characteristics of PV Cell	11
<b>CHAPTER 3 WIND TURBINE ANALYSIS</b>	<b>15</b>
3.1 Wind Turbine Design and Construction	15
3.2 Types of Wind Turbine and its Performance	24
<b>CHAPTER 4 TRANSIENT ANALYSIS OF HYBRID PV/WIND TURBINE AND BUILDING LOAD</b>	<b>30</b>

4.1 System Design and Dynamic Analysis-----	32
4.1.1 Mathematical Model for Photovoltaic (PV) System-----	33
4.1.2 Photovoltaic (PV) Module-----	34
4.1.3 Photovoltaic (PV) Arrays-----	36
4.2 Modeling of Wind Turbines-----	37
4.3 Economic Analysis-----	40
<b>CHAPTER 5 COMPUTATIONAL METHODOLOGY-----</b>	<b>49</b>
<b>CHAPTER 6 RESULTS-----</b>	<b>51</b>
<b>CHAPTER 7 CONCLUSIONS-----</b>	<b>63</b>
<b>LIST OF REFERENCES-----</b>	<b>66</b>
<b>APPENDIX I EQUATIONS FOR PV PANELS-----</b>	<b>70</b>
<b>APPENDIX II SOLAR ENERGY-----</b>	<b>74</b>
<b>APPENDIX III KEY PARAMETERS RELATED TO WIND TURBINES-----</b>	<b>92</b>

## ABBREVIATIONS AND ACRONYMS

A	Annuity of capital investment
ACH	Air change equivalent to the volume of the building per hour, $\text{ft}^3/\text{hr}$ ( $\text{m}^3/\text{s}$ )
$C_e$	Cost of electric energy consumption (cents/kWh)
$C_{ep}$	Cost of electric power produced (cents/kWh)
$C_{ed}$	Cost of excess electric power demand (\$/yr)
$C_{htg}$	Annual cost of space heating (\$/yr)
$C_{opr}$	Total annual cost of building operations (\$/yr)
$C_{pv}$	Capital cost of PV panel (\$/panel)
$C_{wt}$	Capital cost of wind turbines (\$)
Ets	Equivalent total subsidies (%)
$E_{dL}$	Electrical power demand limit (kW)
$E_{ann,pv}$	Annual electric energy produced by the PV per panel (kWh/yr/panel)
$E_{ann,wt}$	Annual electric energy produced by wind turbine per contacted unit (kWh/yr)
$E_{st}$	Solar energy incident on tilted surface/panel at standard conditions, (1000 $\text{W}/\text{m}^2$ )

$E_{tt}$	Total solar energy incident on tilted surface/panel ( $\text{W/m}^2$ )
HVAC	Heating, ventilating and air-conditioning system
$i$	Blended interest rate per annum
$I$	Current developed by the PV module/panel flowing through the load (A)
$I_D$	Diode current (A)
$I_L$	Light current (A)
$I_{sh}$	Shunt current (A)
$I_{mp}$	Current developed by the PV module/panel at maximum power point operation (A)
$I_{sc}$	Current developed by the PV/panel at short circuit conditions of operation (A)
$n$	Life of PV panels or wind turbines (yrs)
$N_{pv}$	Number of PV panels
$N_{tu}$	Number of wind turbine units
$P$	Principal amount or capital cost of the PV panels and wind turbines
$P_{ed}$	Peak electric demand for a given month (kW)
PB	Simple payback period (yrs)



$q_{\text{heat}}$	Heat capacity output of the heat pump, Btu/hr (kW)
$q_{\text{lat}}$	Latent cooling capacity of the heat pump, Btu/hr (kW)
$q_s$	Sensible cooling capacity of the heat pump, Btu/hr (kW)
$q_{\text{tot}}$	Total cooling capacity of the heat pump, Btu/hr (kW)
$R_{\text{load}}$	Load resistance ( $\Omega$ , ohms)
$R_s$	Series resistance ( $\Omega$ , ohms)
$R_{\text{sh}}$	Shunt resistance ( $\Omega$ , ohms)
$t_i$	Moist air temperature of indoor air, °F (°C)
$t_a$	Outside air temperature, °F (°C)
$t_{\text{wi}}$	Wet-bulb temperature of indoor air blowing over the evaporator coil of the air conditioner or heat pump, °F (°C)
$T_c$	Cell operating temperature (°C)
UPF	Utility payback factor
V	Voltage developed by the solar PV panel across the load (V, volts)
$V_{\text{oc}}$	Open circuit voltage developed by the solar PV module/panel (volts)
$V_{\text{mp}}$	Voltage developed by the solar PV module/panel at maximum power point of operation (V, volts)

$V_w$	Measured values of outside air wind velocity, (m/s)
$W_{aux}$	Power supplied to the auxiliary fans (kW)
$W_c$	Power supplied to the compressor of heat pump (kW)
$W_{eqm}$	Power supplied to the equipment, computers (kW)
$W_{light}$	Power supplied to the lights (kW)
$W_p$	Power produced by the wind turbine unit (kW)
$W_{pv}$	Power produced by a PV panel (kW)

### GREEK LETTERS

$\alpha_0$	Module current temperature coefficient ( $A/^{\circ}C$ )
$\beta_0$	Module voltage temperature coefficient ( $A/^{\circ}C$ )
$\eta_{inv}$	Efficiency of the inverter
$\eta_c$	Efficiency of conversion

## LIST OF TABLES

Table 3.1 Wind Power Density Classes -----	16
Table 3.2 GE Wind Turbine Technical Data [GE energy]-----	27
Table 3.3 Vestas V52 850-kW specifications [Vestas]-----	28
Table 3.4 Bergey 10 kW Excel Wind Turbine [Bergey]-----	29
Table 4.1 Basic Specification of Polycrystalline Photovoltaic (PV) Panel-----	35
Table 4.2 Characteristics of 220 W polycrystalline photovoltaic (PV) panel-----	36
Table 4.3 Basic Economic Data of Wind Turbines-----	39
Table 4.4 Basic economic data of PV Panel-----	47
Table 6.1 Evaluation of Zero-Electrical Energy Building (ZEEB) with Hybrid PV Panel and Wind Turbine Systems for Various U.S Cities-----	59
Table 6.2 Evaluation of Zero- Energy Building (ZEB) with Hybrid PV Panel and Wind Turbine Systems for Various U.S Cities-----	61

# LIST OF FIGURES

Figure 2.1 Fritts' Solar Cell .....	8
Figure 2.2 Schematic of a Silicon Crystal Lattice Doped with Impurities to Produce <i>n</i> - type and <i>p</i> -type Semiconductor Material .....	10
Figure 2.3 Effect on pn Junction in Sunlight .....	10
Figure 2.4 Design of PV Array.....	11
Figure.2.5. Air Mass is the Ratio of the Length of the Sun's Rays through the Atmosphere When the Sun is at a Given Angle ( $\theta$ ) to the Zenith, to the Path Length When the Sun is at its Zenith. ....	12
Figure 2.6 I-V Curve of the Solar Cell Showing the Sshort Circuit Current .....	13
Figure 2.7 I-V Curve of the Solar Cell Showing Open Circuit Voltage .....	13
Figure 2.8 Current-Voltage (I-V) Characteristics of a Typical Silicon PV Cell STC .....	14
Figure 3.1 Average Annual Wind Power Across U.S .....	18
Figure 3.2 Blade Pitch Angle Versus Tip Speed Ratio .....	19
Figure 3.3 Three Parameter Characterize the Idealized Power Curve for a Wind Turbine .....	20
Figure 3.4 Power Coefficients for Different Wind Turbine Types .....	21
Figure 3.5 Weibull Distribution Curve .....	23

Figure 3.6 Comparison of Power Coefficient for Common Rotors as per Betz Law -----	23
Figure 3.7 Wind Energy Distribution Based on Betz Limit-----	24
Figure 3.8 Horizontal and Vertical Axis Wind Turbine -----	24
Figure 3.9 (a) Power Curve (b) Wind Turbine (1.5 MW) -----	25
Figure 3.10 Power Versus Wind Speed for a Vestas V52 850-kW (b) Vestas Wind Turbine -----	26
Figure 3.11 Power Versus Wind Speed for a Bergey 10 kW Excel wind turbine (b) Bergey Wind Turbine -----	29
Figure 4.1 (a) Stand Alone PV System -----	30
Figure 4.1 (b) Grid Connected PV Power System -----	31
Figure 4.2 Equivalent Electric Circuits of a Photovoltaic Cell/ Module/ Array -----	33
Figure 4.3 Selection of Location -----	43
Figure 4.4 Selection of Building Envelope Type -----	44
Figure 4.5 Peak Building Load -----	45
Figure 4.6 System Selection -----	46
Figure 4.7 Calculation for Required Number of PV Panel-----	46
Figure 4.8 Estimation for ZEEB and ZEB-----	47
Figure 5.1 Computation Methodology of TABLET -----	50
Figure 6.1 Variation of PV and Wind Power for Various Cities -----	53

Figure 6.2 Variation of Electric Power Cost, Heating, Cooling Load, and Payback Period for Various Cities in US for Zero-Electrical Energy Building -----	53
Figure 6.3 Variation of Electric Power Cost for Various Cities in US for Zero-Electrical Energy Building -----	53
Figure 6.4 Variation of Cooling load, Annual Cost of Operation and Number of PV Panels Required with Lighting Load for Various Cities in US for Zero Energy Cost Building -----	54
Figure 6.5 Variation of COP, Heating Capacity and Compressive Power with Temperature of Outside Air -----	54
Figure 6.6 Variation of Number of PV Panels and Wind Turbine Units for Various Cities in US for ZEEB and ZEB-----	54
Figure 6.7 Variation of Total Capital Cost of PV, Hybrid and Wind Turbine Units for Various Cities in US for ZEEB and ZEB -----	55
Figure 6.8 Variation of Cost of Electricity produced from PV, Hybrid and Wind Turbine Units for Various Cities in US for ZEEB and ZEB-----	55
Figure 6.9 Variation of Payback Period with PV Cost and Utility Payback Factor (UPF) -----	55
Figure 6.10 Variation of Payback Period with Cost of PV Panels and Rate of Subsidies	56
Figure 6.11 Variations of PV Panels, Capital Cost. Electricity Cost and Payback Period for Various Cities in US for Zero-Electric Energy Building -----	56

Figure 6.12 Variations of PV Panels, Capital Cost. Electricity Cost and Payback Period of  
Hybrid System for Various Cities in US for Zero-Electric Energy Building 56

Figure 6.13 Variations of Wind Turbine Units, Capital Cost, Electricity Cost and Payback  
Period of Wind Power System for Various Cities in US for Zero-Electric  
Energy Building -----57

Figure 6.14 Variations of PV Panels, Capital Cost. Electricity Cost and Payback Period  
for Various Cities in US for Zero Energy Building -----57

Figure 6.15 Variations of PV Panels, Capital Cost. Electricity Cost and Payback Period of  
Hybrid System for Various Cities in US for Zero Energy Building -----58

Figure 6.16 Variations of Wind Turbine Units, Capital Cost, Electricity Cost and Payback  
Period of Wind Power System for Various Cities in US for Zero Energy  
Building -----58

# CHAPTER 1

## INTRODUCTION

According to the report from the DOE [1], buildings are the largest energy consuming sector in the United States, accounting for 39% of total energy consumption and 73% of the electricity consumption for meeting the building loads.

### 1.1 Fossil Fuels

Worldwide, annual energy consumption at the end of 2010 is estimated to be about 512 quads [1]. The energy consumption in US was 100 quads for the year 2005, and it is estimated that US will need 103.3 quads by the end of 2010. The US has an annual increase of 3% in energy consumption, and close to 32% and 23% of the energy produced, is used for industrial and residential applications, respectively. Most of the world's electric power is generated by use of fossil and nuclear fuels, and use of fossil fuels, considered by many to be primary cause of greenhouse gases causing global warming. US reserves, as of January 2007 are reported to be 705 trillion cubic feet of natural gas and 338.3 billion barrels of petroleum [1]. The U.S electric power consumption expected to rise from 782 billion kilowatt-hours in 2005 to 797 billion kilowatt-hours by the end of 2010, raising the fear that fossil fuels will be run out

by 2050. Continued use of fossil fuels would increase the emissions of carbon dioxide and other pollutants, thus exasperating the global warming phenomenon. As the emitted gases increases temperatures towards Earth's poles, insects and pests could be migrating with diseases such as dengue fever, malaria which can result in an increase in these



diseases by 10 to 15%. [2] Apart from aforementioned indirect effect of heat, there will be more cases of heatstroke, heart attacks and other ailments provoked by the direct heat caused by global warming. According to EPA, “In July 1995, a heat wave killed more than 500 people in Chicago region” alone [2].

The increasing demand of power will need clean power from renewable resources such as wind, solar, biomass, and geothermal power. Among all the renewable energy sources, wind and solar power have gained a lot more growth compared to their growth in last few years. Recently, greater importance is placed on using the hybrid systems, especially in the remote locations for stand-alone applications.

## **1.2 History of Wind Energy**

Wind power has been in use since the tenth century for applications of water pumping, and grain grinding. At location, where sufficient wind energy exists, a large scale wind turbines have been installed to produce electricity. In the early 1930s, the Russians built a large windmill with a 100 ft diameter blade, but it had very low power conversion efficiency. Vermont utility in the 1940s built a very large scale windmill of rated capacity 1.25 MW at a cost of \$ 1.25 million. This project was abandoned, after one of its blades broke down due to fatigue failure.

NASA (National Aeronautics and Space Administration) entered into the wind power industry market with a wind power unit of 100 kW capacity at a cost of a million dollars. Concerns on environmental air quality during the 1980s, forced the energy industry for greater use of wind turbines to produce electricity. The design and successful operation of a large scale wind turbines encountered several challenges in reducing their capital costs,

and ensuring smooth operations due to lack of constant angular velocity and torque that can produce the A.C power. It was difficult to achieve these features with wind turbines, as the wind blows with various velocities in different directions at a given location. Superior blade design shapes and tower configurations and materials achieved in the early 2000s, enabled rapid growth in wind power installations. At present, the cost of electricity produced from wind turbines is lower than 2.7cents/kWh in locations of high wind potential.

### **1.3 History of Photovoltaics**

Apart from wind energy, solar energy is also abundantly available on Earth. The solar energy falling on Earth in a year is ten thousand times more than the existing fuel sources available on Earth. The elements such as silicon, germanium etc. used in making the PV cell is also copiously available on Earth. The PV cells can be classified as pollution-free as they do not produce any by-products that may contribute towards air/water pollution and also do not contain any moving parts that may cause noise pollution. The first PV cell introduced to the world was described in a paper dated back in 1877 [3]. In 1883, Charles [3] constructed a selenium solar cell, which was as popular as the silicon PV cell used today. During the early days, the efficiency of a solar cell, which is defined as the percentage of the solar energy falling on the surface of the PV cell, which was converted into electricity, was almost 1%.

During the first half of the twentieth century, the Chaplin-Fuller-Pearson team [3] developed a new PV cell made up of semiconductors. In the early 1950s, they utilized silicon slices in producing the PV cells and they succeeded in getting the efficiency up to

6%. After further research, the efficiency of the current PV cells available in the market went up to 17%

#### **1.4 Hybrid Systems**

As both wind turbine and PV cells use renewable energy resources to generate electricity, the benefit of combining them into a single system can be significant. The combined system of PV cells and wind turbines is typically referred to as a hybrid system. In addition, the battery system, diesel engine or micro-hydro systems can also work in parallel with such hybrid system to meet the load requirements. In the past, most studies on wind turbine and photovoltaic generation system have considered only one system as a standalone resource. However, research focus has been shifted towards aforementioned hybrid system in recent times and various studies on hybrid system of PV and Wind Turbine with diesel or battery back-up for additional electricity supply can be found in the literature [4].

A few papers were published in 90's that deals with optimizing the size of a hybrid system consisting of wind turbine and photovoltaic panels. Gavanidou [5] and Bakirtzis have considered a trade off method for a resort hotel [5]. Castle et al [6] used a least squares algorithm to design a hybrid wind/PV system for site in Nevada. These studies considered an average annual load profile that exceeded the power demand of a small ranch.

Bansal et al [7] presented important design factors to be considered such as site requirements, problems related to the grid connections, choice of generators, two or three blade rotors, weight, and size considerations and environmental issues for wind energy

conversion systems. Ibrahim et al [8] have presented a review on energy storage techniques that have been employed recently and those that are under development. They discussed characteristics of different electric storage techniques and their field of application. The characteristics such as short term storage, long term storage, maximum power required would determine the most appropriate methods for each type of application. Ashok [9] discussed a method for the life cycle optimization of the entire system. The system includes diesel engine and battery used for backup supply during the energy short fall. It is indicated in this study that each of above system's size and operations were interdependent.

Diya et al [10] presented the techno-economical optimization of a hybrid PV and wind turbine system based on various meteorological conditions. This investigation considered five different sites and compared the individual performance of each site. In this study by Diya et al [10], they considered battery storage for stand-alone photovoltaic without any grid connection. Earlier efforts [11-13] focused on optimum design for standalone applications without consideration of the building loads tied to the PV/Wind systems.

In the past, detailed cost analysis of the hybrid system has not been considered with existing utility cost structure for building optimization. The present study focuses on the optimization of the hybrid system of PV panels and the wind turbines to make a given building a ZEEB or ZEB.

In this investigation, dynamic analysis of the grid-connected hybrid system of photovoltaic (PV) panels and wind turbines has been performed for a light commercial

building. For a building of specified characteristics and load profile, technical and economic evaluation through computer simulations has been conducted for a grid connected hybrid system of photovoltaic (PV) panels and wind turbines. The application of hybrid solar-wind power generation system has been studied by using the long term weather data obtained from the NREL website for six different cities in U.S.

## **CHAPTER 2**

### **PHOTOVOLTAIC ANALYSIS**

Solar energy in one form or the other form is the source of all renewable resources energy on the earth. It is the radiant light or heat emitted from the sun that has been used since ancient times in various ways. For example, biomass is formed from the Sun's energy due to photosynthesis process; wind energy exists due to uneven heating of earth by sun and also due to the rotations of the earth. Solar energy can be used through solar concentrators or heliostats to generate steam or vapor at high temperature and pressure to expand in turbines to produce electricity.

Photovoltaic or solar cell is a device when exposed to sun, converts solar energy directly into the electricity. The PV cell is mostly made from silicon; it emits no harmful gases and has no moving parts and hence produces pollution free, noise free electricity as its output.

#### **2.1 A Brief Glance at History of Photovoltaic:**

The term “photo” comes from the Greek word meaning “light” and the word “voltaic” was named after the Italian physicist Count Alessandro Volta, the inventor of battery, which means “electric”. Hence, Photovoltaic describes the flow or generation of electric current from light. The photovoltaic effect was first observed by the French physicist Alexandre-Edmond Becquerel, who presented a paper in 1839 [3] describing his

experiments with a 'wet cell' battery, in which he found that the battery voltage increased as its silver plates were exposed to the sunlight.

The first solar cell was constructed in 1883 by a New York scientist named Charles Edgar Fritts. He made a selenium solar cell similar to the

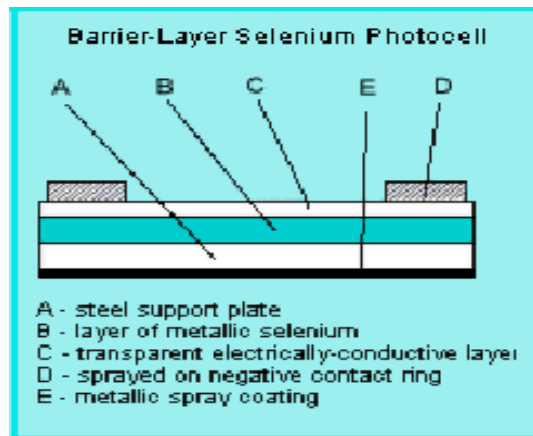


**Figure 2.1** Fritts' Solar Cell [14]

silicon solar cell of today, which consisted of thin wafers of selenium covered with very thin, semi transparent gold wires and a protective sheet of glass. But, his solar cell had very low efficiency. The efficiency is defined as the fraction of energy falling on the cell that is converted to electricity. This solar cell achieved an efficiency of less than 1%. For many years, scientists worked on solar cells to improve the efficiency by taking material characteristics in consideration and the breakthrough occurred in 1950s that set in the motion the development of the modern, high efficiency solar cells. All these experiments were done at the Bell Telephone Laboratories (Bell Labs) in New Jersey, USA, by Darryl

Chapin, Calvin Fuller and Gerald Pearson with their co-scientists. They were doing research on the effect of light on semi-conductors.

### **2.1.1 Semi-Conductors**

Semiconductors are non-metallic materials that lie between conductors and insulators. Conductors offer very little resistance to the flow of current through it. On the other hand, insulators block the flow of current through it. Hence, the materials whose electrical characteristics lie between them are called semi-conductors.

The atoms of every element are held together by the bonding action of valence electrons. This bonding is due to the fact that it is the tendency of each atom to complete its last orbit by acquiring 8 electrons in it. However, in most of the substances, last orbit is incomplete. This makes the atom active to enter into other orbit by losing, gaining or share valence electrons with other atoms. [15]

There are many semi-conductors available in the market but very few of them have a practical application in electronics. The electrical conductivity of a semiconductor changes appreciably with temperature. At room temperature, thermal energy breaks some of the covalent bonds of semi-conductors. This will make some electrons free and these electrons will make a tiny electric current. The breaking of the covalent bond of semi-conductors has left it with the deficiency called a “hole”. This hole becomes filled by the other neighborhood electrons and leaves behind another hole. There will be free electrons and holes in the semi-conductor and free electrons will move towards positive terminal, and holes will drift towards negative terminal if potential difference is applied across the semi-conductors.



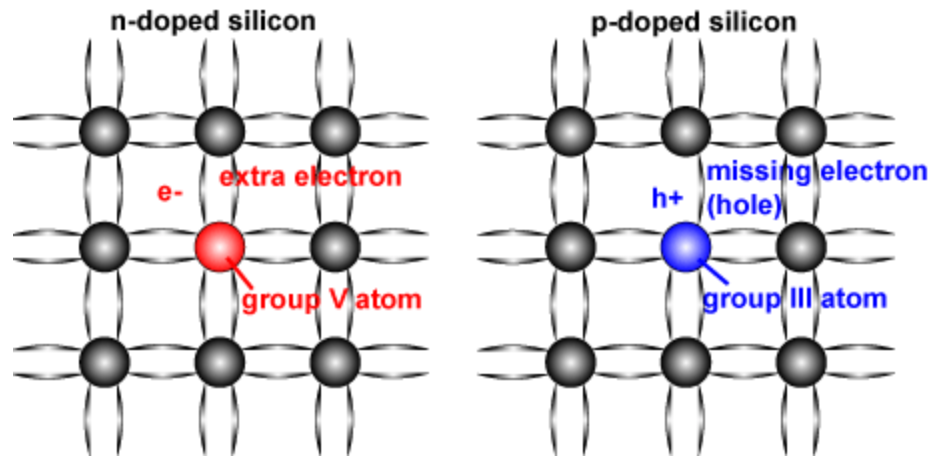


**Figure 2.2** Schematic of a silicon crystal lattice doped with impurities to produce *n*-type and *p*-type semi-conductor material [16]

A semi-conductor in an extremely pure form is known as intrinsic semi-conductor. They have very little conductivity at room temperature, which can be increased by the addition of a small amount of suitable metallic impurity. Depending upon the impurities added they are classified as *n*-type and *p*-type semiconductors. Current conduction in a *p*-type semiconductor is predominantly by holes and in an *n*-type it is by electrons. So when a *p*-type and *n*-type semi-conductors are joined then the contact surface is called *p*-*n* junction.

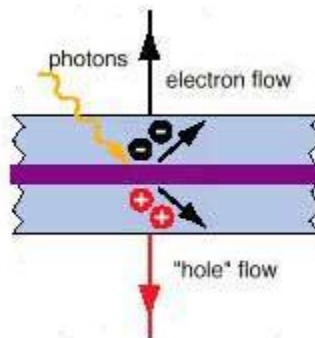


**Figure 2.3** Effect on *p*-*n* junction in sunlight [17]

When p-n junction is kept in the sunlight, the photons will free the electrons in n-type and hence, current will flow. As shown in Figure 2.3. A single p-n junction of semi-conductor is called a PV cell and a module consisting of several cells, or an array consisting of several modules, while an array represents a group of panels as shown in Figure 2.4

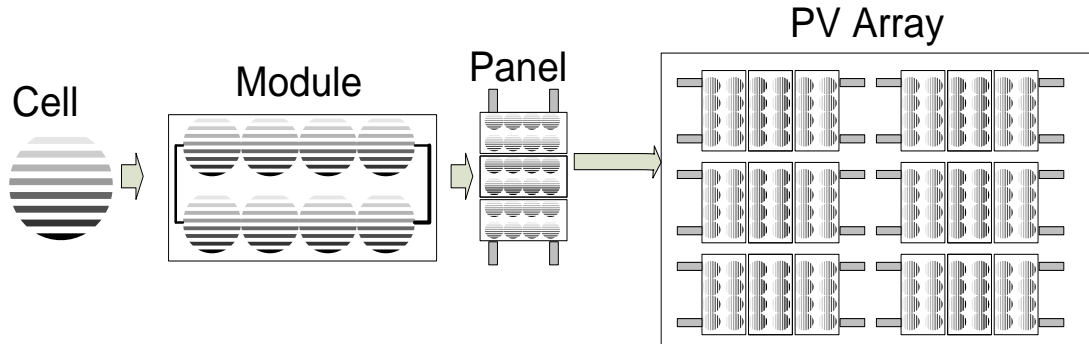


**Figure 2.4** Design of PV array

## 2.2 I-V Characteristics of a PV Cell

The photovoltaic panels are made from combination of several PV modules placed in series and parallel to produce electricity with available insolation to meet the electrical load demand at required voltage and current. In selection of PV panels, it is necessary to estimate the performance or power output of several PV panel placed in the market. For that purpose, power output (W) of various panels is expressed for the same input conditions called at uniform standard conditions. The standard input conditions are characterized by the variables such as solar flux,  $G_T$  ( $\text{W}/\text{m}^2$ ), the ambient temperature,  $T_a$  ( $^\circ\text{C}$ ), the air mass (AM), while the output conditions are the output voltage,  $V$  (Volt), the output current,  $I$  (Amp) and the output power,  $P_{pv}$  (W).

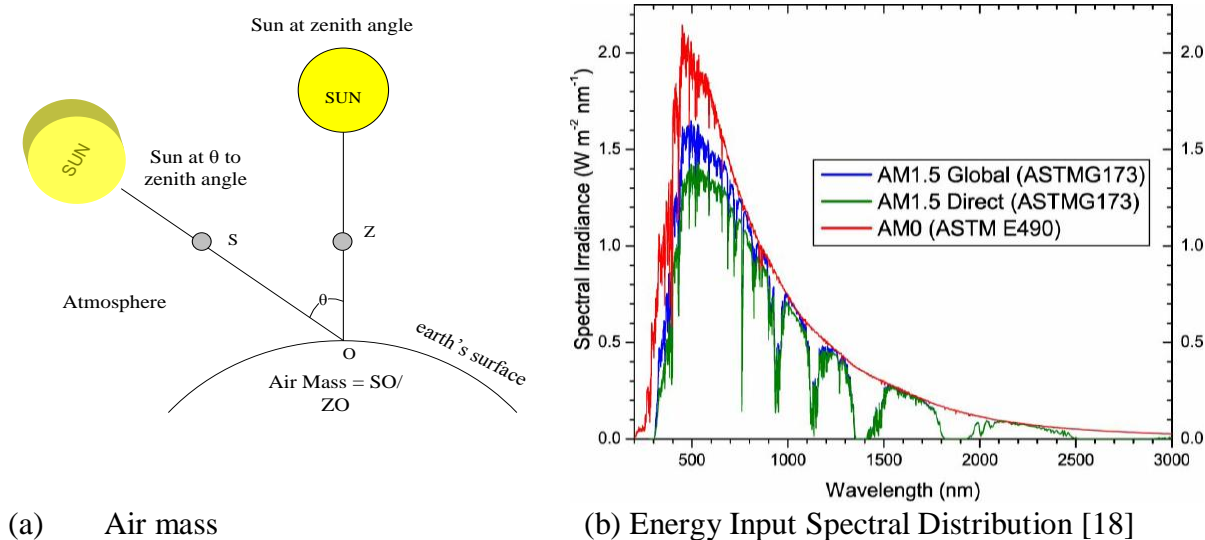


**Figure.2.5.** Air Mass is the ratio of the length of the sun's rays through the atmosphere when the sun is at a given angle ( $\theta$ ) to the zenith, to the path length when the sun is at its zenith.

The air mass ratio AM is the ratio of the path length (SO) of the sun's rays through the atmosphere when the sun is at a given angle ( $\theta$ ) to the zenith, to the path length (ZO) when the sun is at its zenith as shown in Figure 2.5(a).

The variation of the spectral distribution of the energy output with air mass is shown in Figure 2.5(b). Current-voltage (I-V) characteristic of a typical PV module are shown in the Figure 2.6. This characteristic shows two key parameters called "Short Circuit Current" and the "Open Circuit Voltage".

**Short Circuit Current:** It is the current produced in the cell, when the voltage across the solar cell is zero, as seen in Figure. 2.6

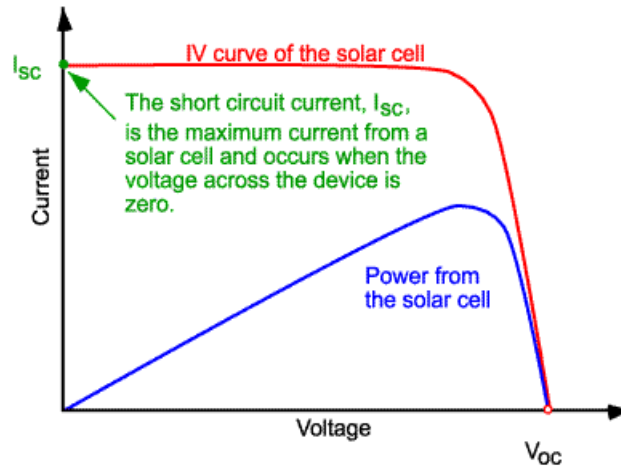


**Figure 2.6** I-V Curve of the solar cell showing the short circuit current [16]

**Open Circuit Voltage:** It is the voltage developed across the cell, when the current flowing through the circuit is zero, as seen in Figure 2.7

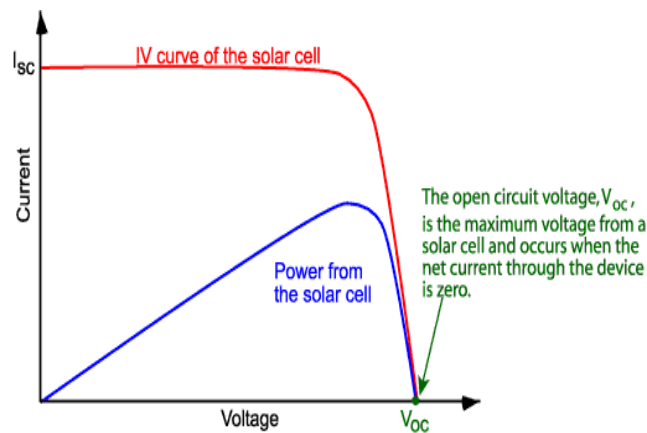
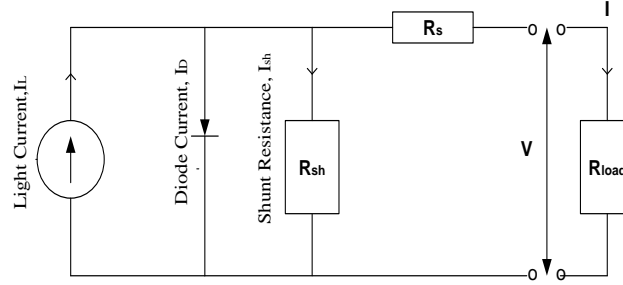
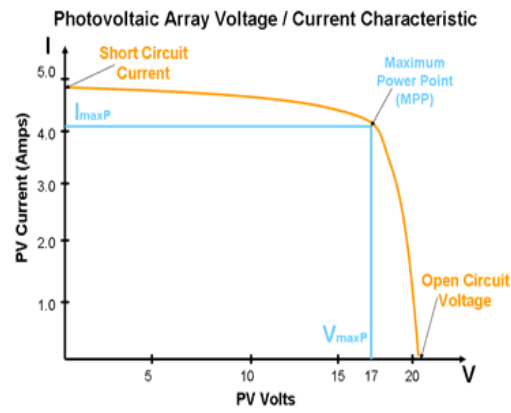


**Figure 2.7** I-V curve of the solar cell showing open circuit voltage [16]

The Figure 2.8(a) shows an equivalent electrical circuit for a single cell under Standard Test Condition (STC) and the Figure 2.8(b) shows the corresponding output current and voltage of PV cell.



(a) PV cell under STC



(b) I-V diagram

**Figure 2.8** Current-voltage (I-V) characteristics of a typical silicon PV cell STC

The variation in voltage and current for a typical PV cell is shown in Figure 2.8(b). The point of short circuit current is when the current is maximum ( $I_{sc}$ ) and the point of open circuit voltage is where the voltage is maximum ( $V_{oc}$ ). Any point between these two points, the current ( $I$ ) and voltage ( $V$ ) would be less than  $I_{sc}$  and  $V_{oc}$  respectively. The product of  $V$  and  $I$  represents the power ( $P = VI$ ) produced by the PV cell. However, there exist a point of operation between these two parameters of  $I_{sc}$  and  $V_{oc}$ , where the magnitude of  $P$  is maximum called Maximum Power Point (MPP) as shown in Figure 2.8(b).

## **CHAPTER 3**

### **WIND TURBINE ANALYSIS**

The increasing energy demand and the need for clean power have been directing everyone's attention to the sources of renewable energy resources. These alternative energy sources are pollution free, abundantly available, and practically unlimited. Wind is one of the renewable energy resources, which can be converted into the useful energy. Wind turbine converts the kinetic energy of wind into mechanical shaft power. If the mechanical energy is directly used by devices such as pumps and grinding stones, it is known as a windmill rather than wind turbine. If the wind energy is converted into electricity, the machine is called a wind generator or wind turbine.

#### **3.1 Wind Turbine Design and Construction**

Wind turbine works at their best when working under unrestricted wind access to wind speeds. Currently, the wind power industry is experiencing a rapid growth in the world. The electricity can be produced continuously in areas, of high wind velocities. At the peak demand load, when the PV system is not able to meet the load, the wind turbine can be used in hybrid mode to meet the peak load. A hybrid system consisting of wind turbine/s and photovoltaic panels with diesel generator or battery bank as a backup power supply are employed for stand-alone applications, especially in remote areas far away from the grid network. The wind industry classified the wind energy potential into seven classes as shown in Table 3.1. The potential sites with wind class lower than 3 ( $V_w < 5.1$  m/s or 11.5 mph) are not suitable for wind power development.

**Table 3.1** Wind Power Density Classes

Wind Power Class	10 m (33) ft		50 m (164 ft)	
	Wind Power Density (W/m <sup>2</sup> )	Speed m/sec (mph)	Wind Power Density (W/m <sup>2</sup> )	Speed m/sec (mph)
<b>1</b>	0	0	0	
<b>2</b>	100	4.4 (9.8)	200	5.6 (12.5)
<b>3</b>	150	5.1 (11.5)	300	6.4 (14.3)
<b>4</b>	200	5.6 (12.5)	400	7.0 (15.7)
<b>5</b>	250	6.0 (13.4)	500	7.5 (16.8)
<b>6</b>	300	6.4 (14.3)	600	8.0 (17.9)
<b>7</b>	400	7.0 (15.7)	800	8.8 (19.7)
	1000	9.4 (21.1)	2000	11.9 (26.6)

However, at a given location the wind velocity, increases with height from the ground according to the shear law

$$\frac{V_w}{V_{w0}} = \left( \frac{H}{H_0} \right)^{\frac{1}{7}} \quad 3.1$$

where,

$V_w$  = velocity of wind at height H

$V_{w0}$  = velocity of wind at height  $H_0$

Figure 3.1 shows the areas with various wind potential across U.S. The detailed maps for a given region can be obtained from NREL website.

The wind velocity is a vector quantity that has a magnitude and direction. Both of these change with time at a given site. A wind turbine of rotor diameter  $D$  will have a swept area  $A$  equal to  $\pi D^2/4$ . The mass flow rate of air passing through the plane of blade rotation can be given as,

$$\dot{m} = \rho A (V_1 + V_2)/2 \quad 3.2$$

where,

$V_1, V_2$  = wind velocities at upstream and downstream of the blades, respectively

$\rho$  = density of the air at the given site

The maximum wind power that can be obtained from the difference in kinetic energy of wind with these two velocities given by,

$$P_m = 0.5 \dot{m} (V_1^2 - V_2^2) \quad 3.3$$

$$P_m = 0.5 [\rho A (V_1 + V_2)/2](V_1^2 - V_2^2) \quad 3.4$$

The above equations can be re written as

$$P_m = 0.5 \rho A \left[1 + \frac{V_2}{V_1}\right] \left[1 - \left(\frac{V_2}{V_1}\right)^2\right] V_1^3 \quad 3.5$$



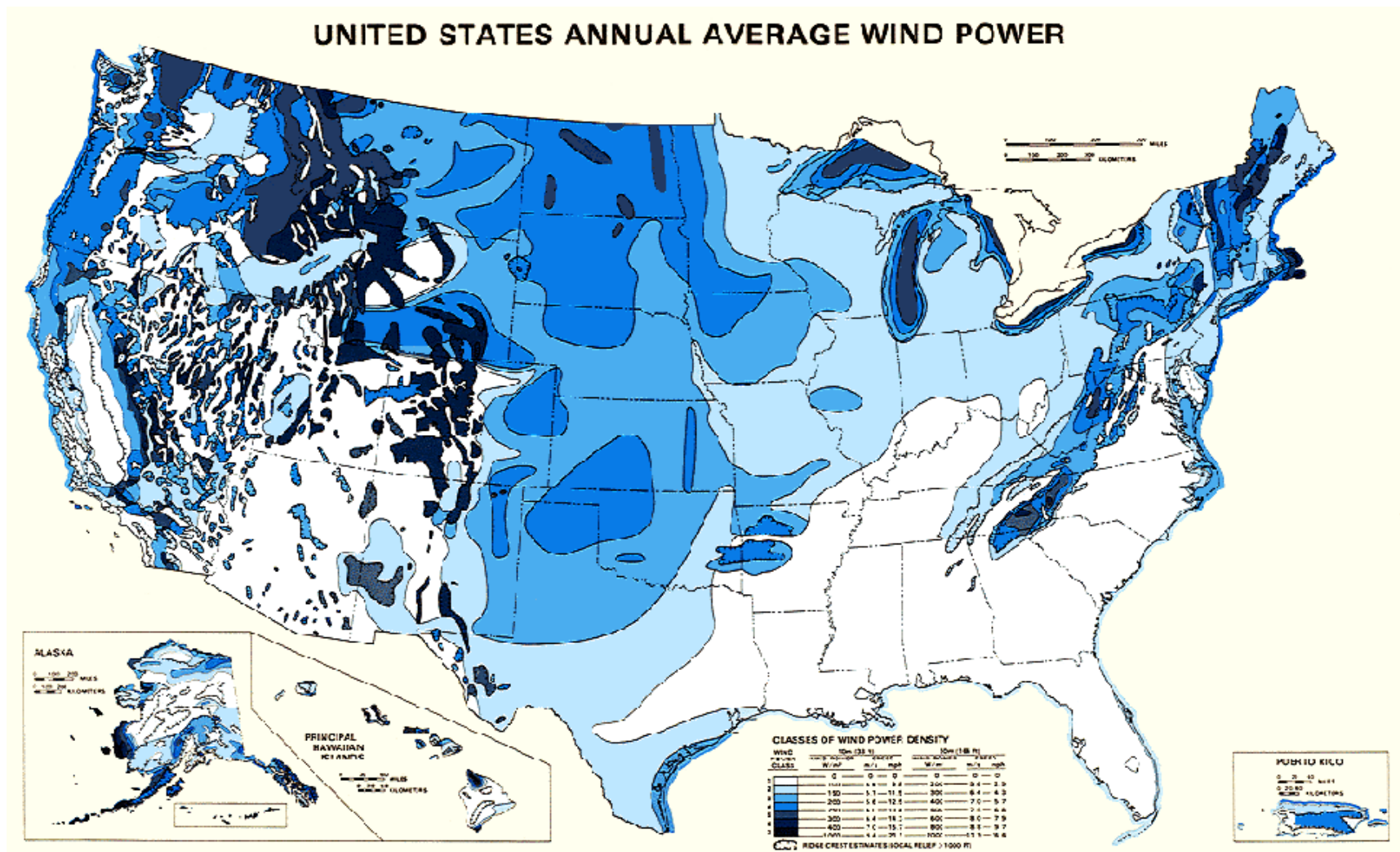


Figure 3.1 Average Annual Wind Power across U.S [NREL]

Or, more compactly as

$$P_m = 0.5 \rho A C_p V_1^3 \quad 3.6$$

where,

$C_p$  = power coefficient of wind turbine given by

$$C_p = (1 + V_2/V_1) [1 - (V_2/V_1)^2] \quad 3.7$$

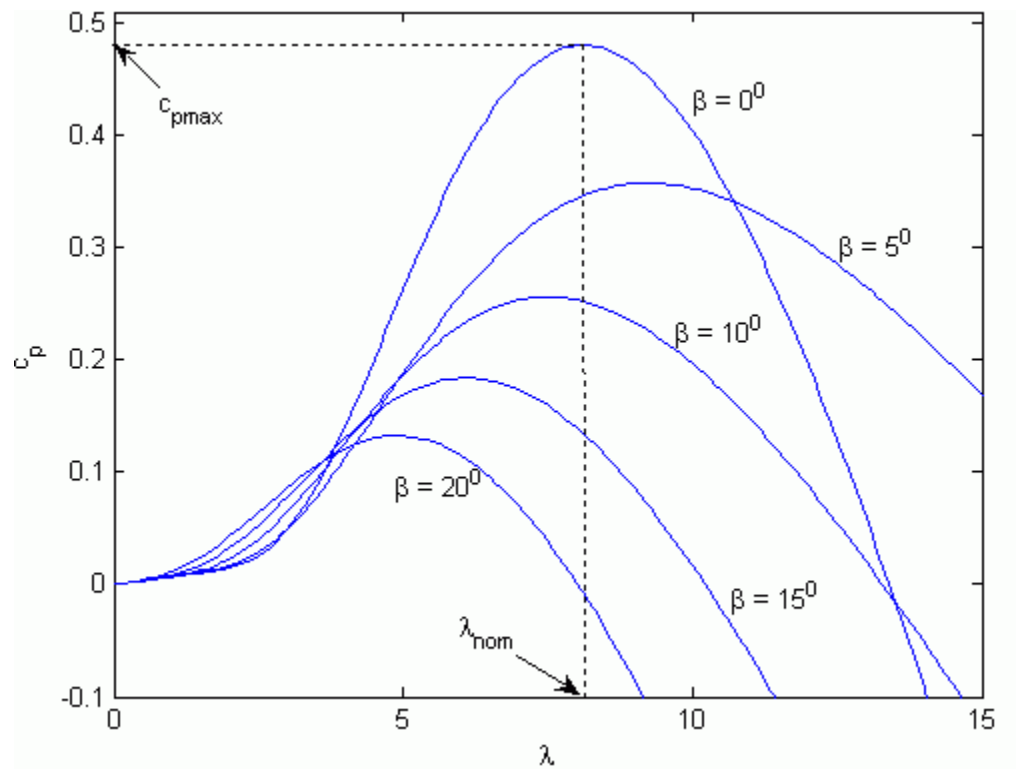


**Figure 3.2** Blade pitch angle versus tip speed ratio

For maximum value of  $P_m$ , the above equations can be differentiated with respect to the ratio of  $V_2/V_1$  that eventually leads to a  $C_{p,max} = 0.5926$ . This maximum value of  $C_p$  is known as Betz limit. The realistic values for  $C_p$  for modern turbines vary from 0.35 to 0.45. Since, the magnitude and direction of wind is transient, the manufacturer of

these devices often seek the maximum  $C_p$  value for these units during operation by varying the blade pitch angle ( $\beta$ ) to match the varying wind conditions. Typically,  $C_p$  varies with blade pitch angle  $\beta$  and another key variable called tip speed ratio  $\lambda$ , which is the ratio of blade tip speed to the undisturbed wind velocity. A typical relationship among these variables is as shown in the Figure 3.2. However most of the manufacturers display the performance of wind turbines only as dependent on single variable, namely the wind speed as shown in Figure 3.3. In this figure, three key wind speeds are also indicated. The cut-in wind speed is the minimum wind speed required to generate useful power, while the cut-out wind speed is the maximum speed above which the operation of wind turbine is not permitted to protect the turbine from heavy wind damage. The rated wind speed is the speed at which rated power is produced by the wind turbine.

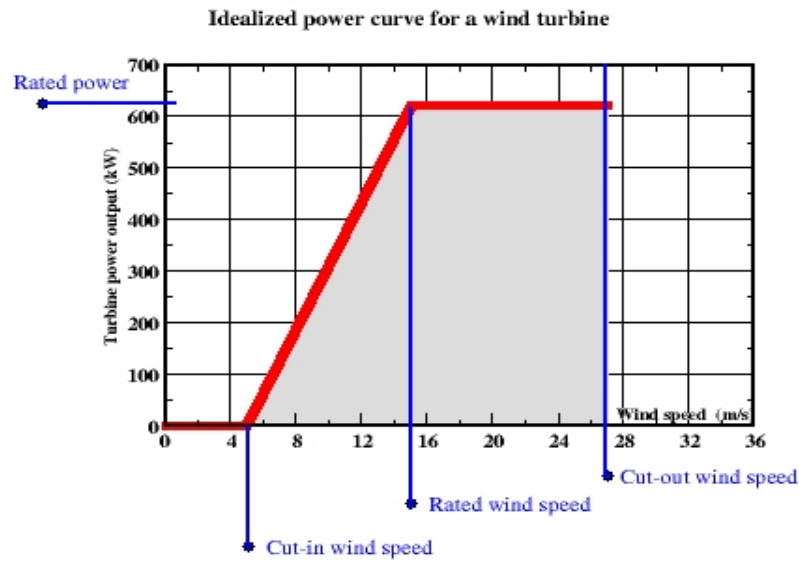


**Figure 3.3** Three parameter characterize the idealized power curve for a wind turbine [20]

From Figure 3.4, it is observed that there is an optimum point available for each wind turbine at which the  $C_p$  reaches a maximum value. This is useful for control purposes because in maximizing the power coefficient and hence maximum power from the wind turbine.

**Weibull Distribution:** Turbine designer needs the information to optimize the size of wind turbine, so as to minimize the generating cost or maximum power from it. In such a case, they need to measure the wind speeds for particular site throughout a year. But, wind variation for any site can be given by the Weibull distribution as shown in Figure 3.5. This particular site has a mean wind speed of 7 m/s and, the shape of the curve is determined by two parameters called scale factor ( $c$ ), and the shape factor ( $k$ ).

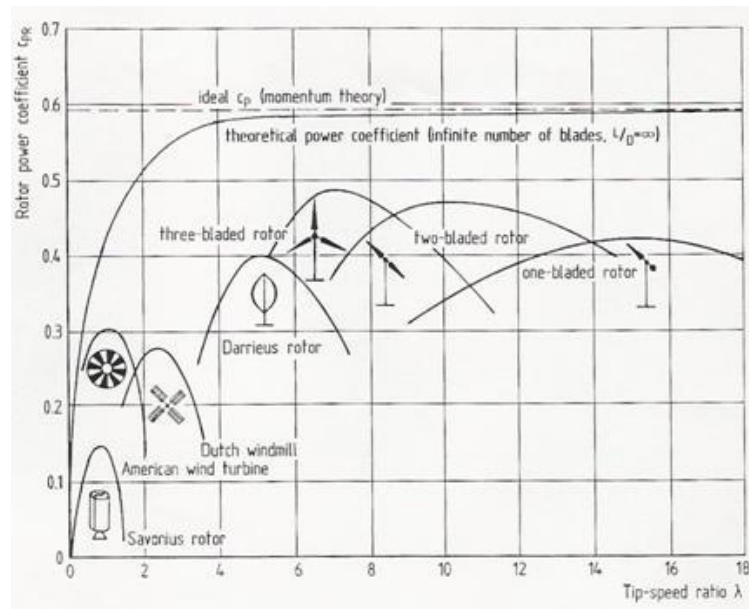


**Figure 3.4** Power coefficients for different wind turbine types [21]

When the wind speed is lower than 3 m/s (known as a calm period), the power becomes very limited to produce electricity and the system should be stopped. As smaller

cities do not have wind data collected for long years; the Weibull probability distribution has been widely used to describe the wind speed variation for shorter periods. The data are averaged over the calendar months and can be described by the Weibull probability function, given as follows:

$$h(v) = \frac{k}{c} \left(\frac{v}{c}\right)^{k-1} e^{-(v/c)^k} \text{ for } 0 < v < \infty \quad 3.8$$

The Weibull function expresses the fraction of time the wind speed is between  $v$  and  $v + \Delta v$  for a given  $\Delta v$ . In practice, most sites around the world present a wind distribution with  $k$  (shape factor) in the range 1.5 to 2.5. For most of them,  $k = 2$ , a typical wind distribution found in most cities, is also known as the Rayleigh distribution, given by

$$h(v) = \frac{k}{c} \left(\frac{v}{c}\right) e^{-(v/c)^2} \quad 3.9$$

Weibull probability density function (Probability Density Function, pdf),

$$f(v) = \left(\frac{k}{c}\right) \left(\frac{v}{c}\right)^{(k-1)} e^{-(v/c)^k} \quad \text{For } 0 < v < \infty \text{ and } c, k > 0 \quad 3.10$$

Weibull Cumulative distribution function (Cumulative Distribution Function, cdf),

$$f(v) = 1 - e^{-(v/c)^k} \quad \text{For } 0 < v < \infty \text{ and } c, k > 0 \quad 3.11$$

$$\text{Then mean} = E(v) = c \gamma \left(1 + \frac{1}{k}\right) \quad 3.12$$

$$\text{The variance} = V(v) = c^2 \left[ \gamma \left(1 + \frac{2}{k}\right) - \gamma^2 \left(1 + \frac{1}{k}\right) \right] \quad 3.13$$

where,  $\gamma$  = Gamma function. Factor  $c$ , known as the scale factor, is related to the number of days with high wind speeds. The higher the  $c$  is, the higher the number of windy days [22].

**Betz Limit:** The German physicist named Albert Betz calculated that it is not possible to convert 59.3% of the kinetic energy into mechanical energy using any kind of wind

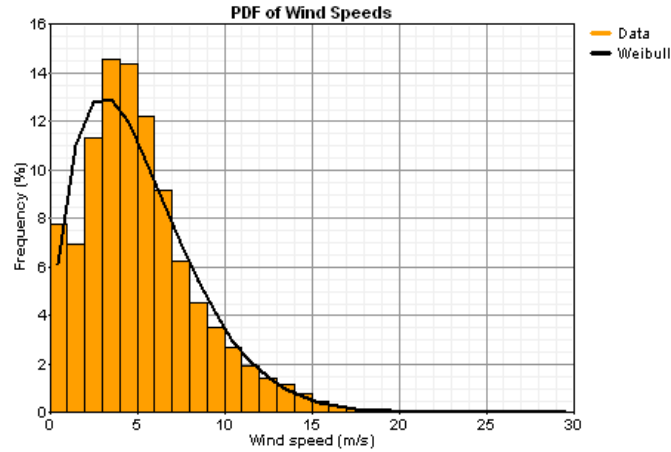


**Figure 3.5** Weibull Distribution Curve [23] turbine.

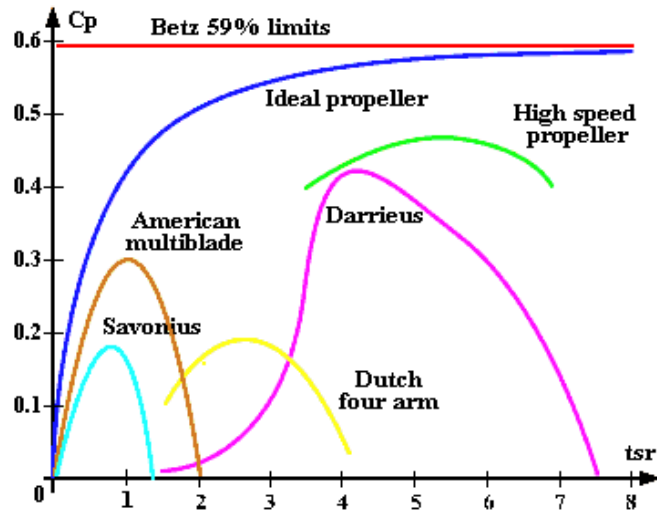


**Figure 3.6** Comparison of power coefficient for common rotors as per Betz law [24]

This is known as the Betz limit, theoretical maximum coefficient of the power for any wind turbine. For better explanation, we can consider the example shown in Figure 3.7.

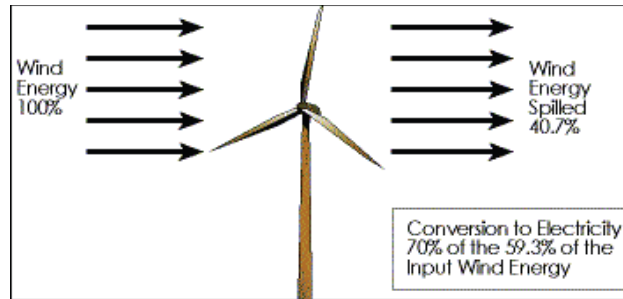


**Figure 3.7** Wind energy distribution based on Betz limit

The above turbine has a capacity to convert 70% of the Betz limit, which amounts to the efficiency of 41%. It is an impressive power coefficient for a given wind turbine. Good wind turbine generally falls in the 35-45% range.

### 3.2 Types of Wind Turbine and its Performance

Wind turbines can be broadly classified based on the axis about which the turbine

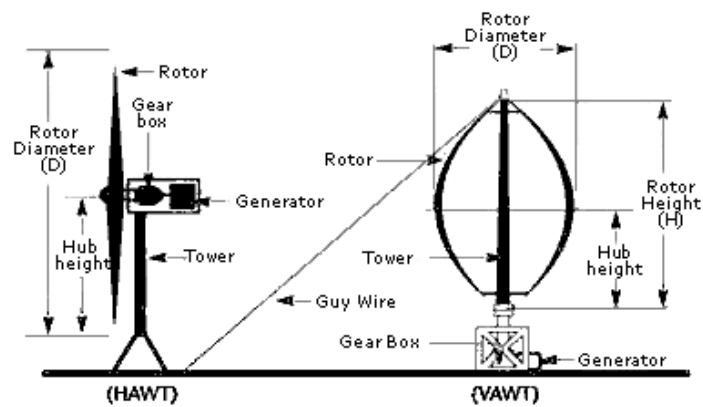


**Figure 3.8** Horizontal and Vertical Axis Wind Turbine [25]

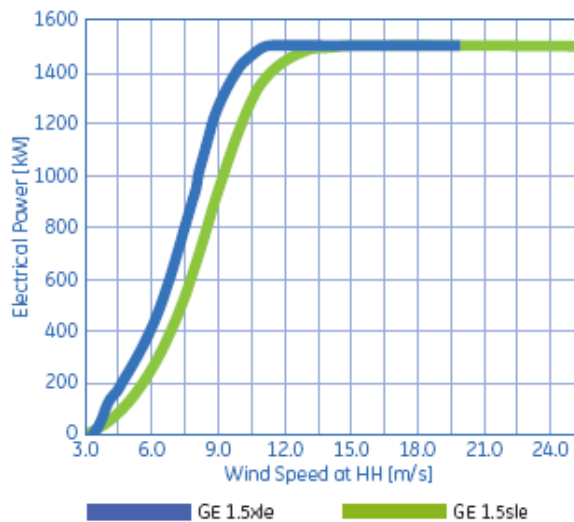
rotor rotates. Most commonly used type is the horizontal axis turbine. Another type is the vertical axis turbine. The Figure 3.8 shows the difference between the aforementioned

types of wind turbines. The horizontal axis wind turbine is also known as upwind turbine in which wind strikes the turbine blades before hitting the turbine tower.

Vertical axis wind turbine is known as the downwind turbine in which the wind strikes the tower before hitting the turbine blades.

For performance of computer simulations by the software TABLET (Transient Analysis of Building Loads and Energy Technologies), we have considered three different kinds of turbines as explained below:

- **GE Energy Wind Turbine (1500 kW):** The power curve and general specification is given below:



(a)



(b)

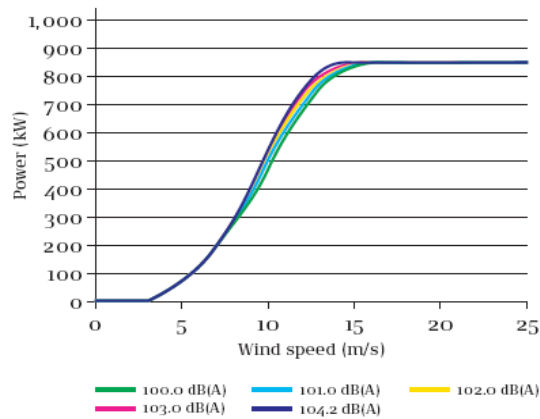
**Figure 3.9** (a) Power Curve (b) Wind Turbine (1.5 MW) [26]



This is the highest power producing wind turbine among three considered. GE model of 1.5 MW is the most efficient in all class because of its high reliability (97%) and capacity factor (48%) compared to the first installed wind turbines [26].

The 1.5 MW turbine has active yaw and pitch regulated with power/torque control capability and an asynchronous generator. It uses a bedplate drive train design where all nacelle components are joined on a common structure, providing exceptional durability. The generator and the gearbox are supported by elastomeric elements to minimize noise emissions. [26] The specifications and power curve are presented in Table 3.2 and Figure 3.9, respectively.

- **Vestas V52 850 kW:** The modest dimensions make the V52 cost effective and easy to transport and install. For its robustness and aforementioned feature we have also considered this unit for computer simulation in TABLET. Technical information on the



(a)



(b)

**Figure 3.10** (a) Power versus wind speed for a Vestas V52 850-kW (b) Vestas wind turbine [27]

V52 850-kW wind turbine is presented in Table 3.3 and photograph is provided in Figure 3.10(b).

**Table 3.2** GE Wind Turbine Technical Data [26]

Operating Data		1.5sle	1.5xle
<b>Rated Capacity:</b>		1,500 kW	1,500 kW
<b>Temperature Range:</b>	<b>Operation:</b>	(-30°C) - (+40°C)	(-30°C) - (+40°C)
<b>Survival:</b>		(-40°C) - (+50°C)	(-40°C) - (+50°C)
<b>Cut-in Wind Speed:</b>		3.5 m/s	3.5 m/s
<b>Cut-out Wind Speed (10 min avg.)</b>		25 m/s	20 m/s
<b>Rated Wind Speed</b>		14 m/s	11.5 m/s
<b>Electrical Interface</b>			
<b>Frequency</b>		50/60 Hz	50/60 Hz
<b>Voltage</b>		690 V	690 V
<b>Rotor</b>			
<b>Rotor Diameter:</b>		77 m	82.5 m
<b>Swept Area:</b>		4657 m <sup>2</sup>	5346 m <sup>2</sup>
<b>Tower</b>			
<b>Hub Heights:</b>		65/80 m	80 m

The power output-wind speed performance is shown in Figure 3.10(a). The performance characteristics in the figure are parameterized in terms of the sound level.

**Table 3.3** Vestas V52 850-kW Specifications [27]

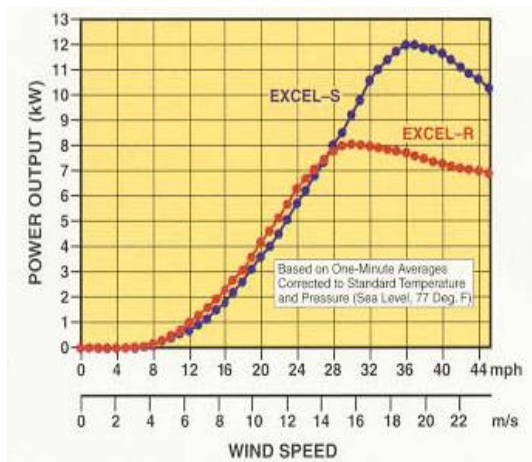
<b>Rated Capacity (kW)</b>	850
<b>Cut-in speed (m/sec)</b>	4
<b>Cut-out Speed (m/sec)</b>	25
<b>Rated wind speed (m/sec)</b>	16
<b>Rotor Diameter (m)</b>	52
<b>Swept area (m<sup>2</sup>)</b>	2124
<b>Rotor speed (RPM)</b>	14-31.4

**Bergey 10-kW Excel:** The first two wind turbines were relatively large wind turbines and used for commercial applications. The Bergey Wind Power Company manufactures small wind turbines suitable for the use in residential and light commercial building applications.

Technical information on the Bergey 10 kW Excel wind turbine is given in Table 3.4 and photograph is shown in Figure 3.11 (b). Figure 3.11 (a) shows the power output-wind speed performance characteristics.

**Table 3.4** Bergey 10 kW Excel Wind Turbine [28]

<b>Rated Capacity (kW)</b>	10
<b>Cut-in speed (m/sec)</b>	3.1
<b>Cut-out Speed (m/sec)</b>	None (furlled at 15.6 m/sec)
<b>Rated wind speed (m/sec)</b>	13.8
<b>Rotor Diameter (m)</b>	6.7
<b>Swept area (m<sup>2</sup>)</b>	35.3
<b>Rotor speed (RPM)</b>	14-31.4



(a)



(b)

**Figure 3.11** (a) Power versus wind speed for a Bergey 10 kW Excel wind turbine (b)

Bergey wind turbine [28]

## CHAPTER 4

### TRANSIENT ANALYSIS OF HYBRID PV/WIND TURBINE AND BUILDING LOADS

There are two types of power supply systems, one is called a stand-alone system and the other is a grid connected system. Stand-alone systems do not rely on grid power. It can be a PV or, wind turbine system or a combination of both the systems. The figures below show the distinctions between the stand-alone and grid connected systems.

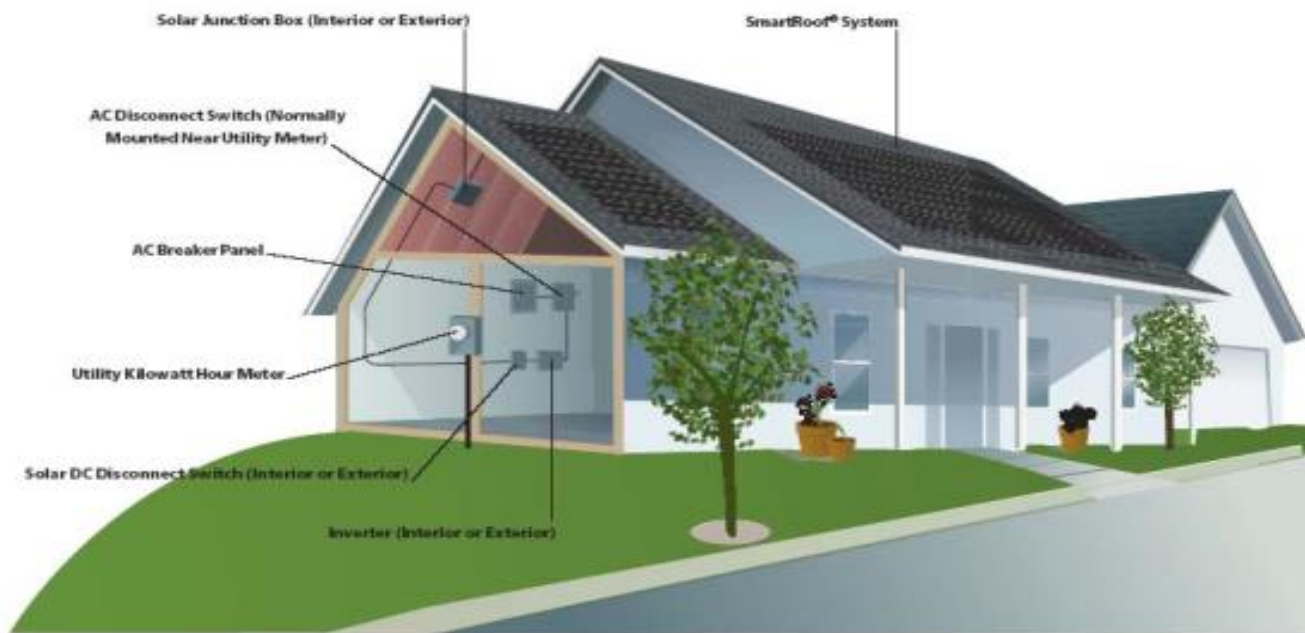


**Figure 4.1 (a)** Stand-alone System [29]

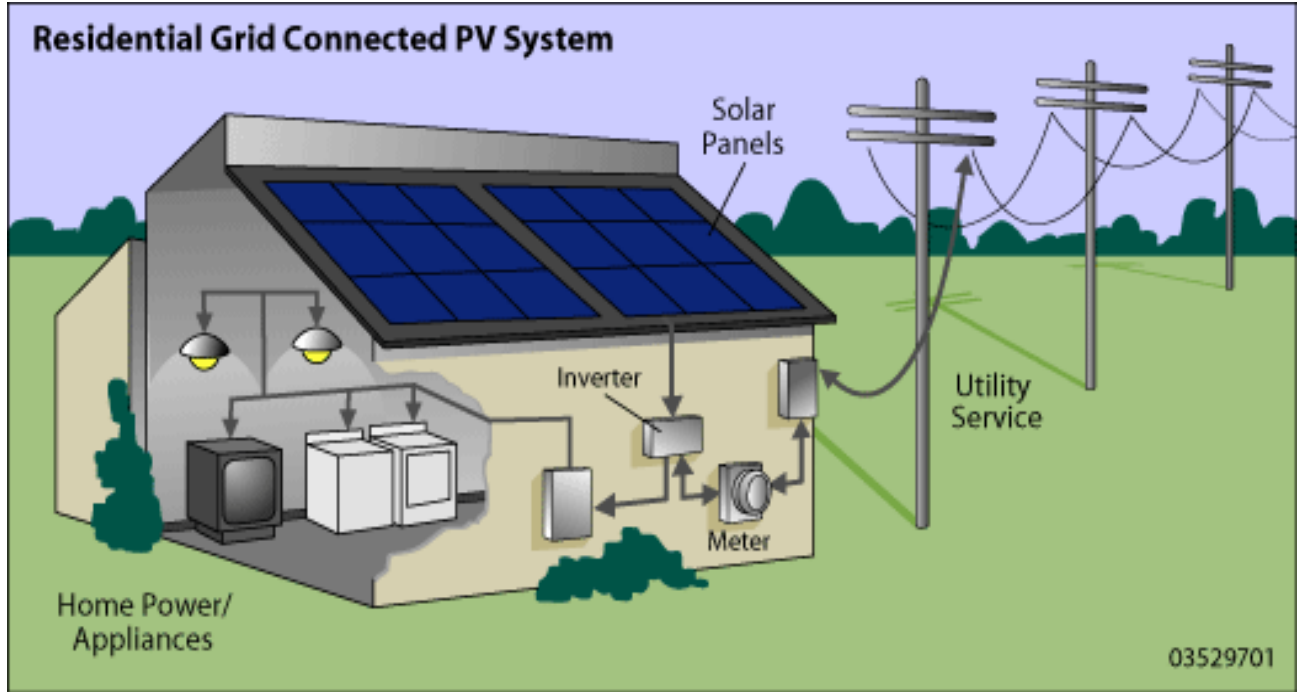


**Figure 4.1** (b) Grid connected PV power system [29]

The stand-alone power system is used primarily in remote areas where utility lines are uneconomical to install due to terrain, other difficulties, or environmental concerns.

Wind and PV power systems have made a successful transition from small stand alone sites to large grid connected systems. Grid connected system supplies power to the site when available, and feeds the grid when excess power exists after meeting the building loads. Two kilowatt-hour meters are used to measure the power delivered to the grid and absorbed from the grid. These two meters are charged differently on a daily or on a yearly basis that allow energy swapping and billing the net annual difference. Generally, utilities pay back twice the amount they charge, in some countries such as in

Germany they pay up to 7 to 8 times the amount per kWh they charge to the customer. Figure 4.1(b) describes the typical residential grid connected PV power system. The higher utility purchase factor (UPF) plays a vital role in reducing the size of the panels or wind turbine systems, thereby reducing the required capital costs and payback periods.

A wind power system may be used for the site where space and aesthetic view are not a big problem. We can even use a small wind turbine in the back side of the house, or on the roof of a tall building. Wind power can be used as a stand-alone or a grid connected system in the same way as a PV power system described above. In order to produce a near constant electric power or a more reliable power supply at a particular site, a combination of the wind and photovoltaic systems can be used. Such system can be installed where wind and solar potential is sufficient to produce electricity by both means economically. In a hybrid system, an optimum size of PV panels and that of wind turbine might provide a minimum cost of electric power generation or a zero-electric energy or zero-energy building.

#### **4.1 System Design and Dynamic Analysis**

In this portion the data pertinent to the evaluated building, the economic data pertinent to the PV panels, and three types of wind turbines, the mathematical models involving key parameters for PV panel, wind turbines, heat pump and other relations are presented. A light commercial building of 10,000 square feet floor area, with 40 occupants, 10 kW of plug in load, an infiltration rate of 0.15 ACH, ventilation rate of 15 cfm, and lighting load of  $1.0 \text{ W/ft}^2$  is assumed. The building roof is made up of 4" concrete with 4.5" of insulation ( $U = 0.036 \text{ Btu/hr.ft}^2 \cdot ^\circ\text{F}$ ) and walls consists of face brick, 8" of concrete and 5" of insulation ( $U = 0.04 \text{ Btu/hr.ft}^2 \cdot ^\circ\text{F}$ ) typically employed for a

medium-sized commercial building with window area of 100 ft<sup>2</sup> on south and north facing walls, in which the occupants work during week days from 8:00 AM to 5:00 PM.

#### 4.1.1 Mathematical Model for Photovoltaic (PV) System

Figure 4.2 shows a typical equivalent electrical circuit that depicts the electrical output of an individual photovoltaic cell, a module consisting of several cells, or an array consisting of several modules.

The shunt resistance  $R_{sh}$ , the series resistance  $R_s$  is in the range from 0.01 to 1.0  $\Omega$ .  $I_L$  is the photon current, which depends upon the light intensity and its wavelength,  $I_D$  is the Shockley temperature-dependent diode current; and  $I_{sh}$  is the PV cell leakage current.

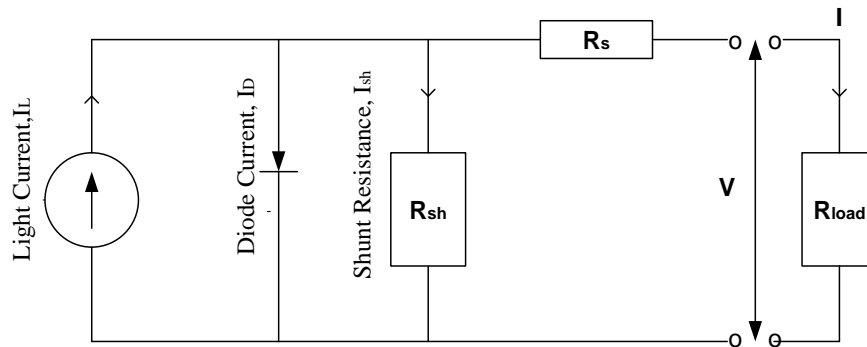


**Figure 4.2** Equivalent Electric Circuits of a Photovoltaic Cell/ Module/ Array

Most of the PV mathematical models are developed using the basic five parameters of the PV modules. However, model involving these five parameters results in non-linear algebraic equations which are very difficult to converge, unless special mathematical algorithms are employed. There is a large set of equations that are to be taken into consideration for output power of a particular panel which ended up into



unsolved set of non-linear equations. It has been an inactive part of this study and documented in Appendix I.

#### 4.1.2 Photovoltaic(PV) Modules

Ai et al. [11] employed a more practical approach by using the measured values of cell temperature  $T_c$  to predict the power output of PV panels. In the present model, a more recent generalized empirical relation for cell temperature as developed by Chenni [12] valid for a freely mounted polycrystalline module is employed.

$$I = I_{sc} \left\{ 1 - C_1 \left[ \exp \left( \frac{V - \Delta V}{C_2 V_{oc}} \right) - 1 \right] \right\} + \Delta I \quad 4.1$$

where,

$$C_1 = \left( 1 - \frac{I_{mp}}{I_{sc}} \right) \exp \left( \frac{-V_{mp}}{C_2 V_{oc}} \right) \quad 4.2$$

$$C_2 = \frac{\frac{V_{mp}}{V_{oc}} - 1}{\ln \left( 1 - \frac{I_{mp}}{I_{sc}} \right)} \quad 4.3$$

$$V = V_{mp} \left[ 1 + 0.0539 \log \left( \frac{E_{tt}}{E_{st}} \right) \right] + \beta_o \Delta T \quad 4.4$$

$$\Delta V = V - V_{mp} \quad 4.5$$

$$\Delta I = \alpha_o \left( \frac{E_{tt}}{E_{st}} \right) \Delta T + \left( \frac{E_{tt}}{E_{st}} - 1 \right) I_{SC} \quad 4.6$$

$$\Delta T = T_c - T_{st} \quad 4.7$$

The cell temperature is obtained from the following empirically determined correlation [12] for the poly-crystal panel.

$$T_c = 0.943 T_a + 0.028 G_t - 1.528 V_w + 4.3 \quad 4.8$$

A **BJ-60P-220 W** polycrystalline solar panel manufactured by B & J Corporation limited with a rated 15% efficiency has been studied here. The physical size of a panel of six cells in parallel each containing ten cells in series is listed in Table 4.1.

**Table 4.1** Basic specification of polycrystalline PV panel

Cell	Polycrystalline Silicon solar cell
	156mm × 156mm
No. of cells and connections	60 (6 × 10)
Dimension of module (mm)	1640 × 992 × 50
Weight	21 kg

The normal operating cell temperature (NOCT) is defined as the cell or module temperature when the cell or module is mounted in their normal way at a solar radiation

level of  $1000 \text{ W/m}^2$ , a wind speed of  $1.5 \text{ m/s}$ , ambient temperature of  $T_a = 25^\circ\text{C}$  and at no-load operation (i.e, with  $\eta_c = 0$ ). A typical Manufacturer's data for a  $220 \text{ W}$  model is given in Table 4.2.

#### 4.1.3 Photovoltaic (PV) Arrays

For practical use, a certain number of PV modules are needed to be connected in parallel/series to meet user's demand on voltage and power. The operating voltage of a system determines the number of ( $M_{PV}$ ) series connection PV modules needed, and the number of parallel

#### Manufacturer' Data for a BJ-60P-220 W Polycrystalline PV panel

**Table 4.2** Characteristics of  $220 \text{ W}$  Polycrystalline PV panel

Open circuit voltage ( $V_{oc}$ )	$36.7 \text{ V}$
Optimum operating voltage ( $V_{mp}$ )	$29.4 \text{ V}$
Short circuit current ( $I_{sc}$ )	$8.31 \text{ A}$
Optimum operating current ( $I_{mp}$ )	$7.48 \text{ A}$
Maximum power at STC ( $P_m$ )	$220 \text{ W}_p$
NOCT	$46^\circ\text{C} \pm 2^\circ\text{C}$
Current temperature coefficient	$0.06 \pm 0.01 \text{ \%}/\text{K}$
Voltage temperature coefficient	$(165 \pm 10) \text{ mV}/\text{K}$

The above electrical characteristics are within  $\pm 10$  percent of the indicated values of  $I_{sc}$ ,  $V_{oc}$ , and  $P_{max}$  under STC.

connection ( $N_{PV}$ ) of PV module string determines the capacity of the PV array. This can be expressed in mathematical terms as follows:

$$P_{PV, SYSTEM} = N_{PV} P_{PV, MODULE} \quad 4.9$$

$$V_{PV, SYSTEM} = M_{PV} V_{PV, MODULE} \quad 4.10$$

Number of Parallel Legs:

$$PL = N_{PV} / M_{PV} \quad 4.11$$

## 4.2 Modeling of Wind Turbines

Wind turbine characteristics are often published by their manufacturers for each of their models placed in the market. These characteristics show the shaft power produced by the wind turbine for different wind velocities. These characteristics also show the cut-in speed and cut-out speeds of their unit on the same graph as discussed in the previous chapter. In this study, three different types of wind turbines are considered according to their rated capacity. Wind turbine I has a rated capacity of 10 kW, so that it can be placed near the building as an independent unit, while wind turbine II has a rated capacity of 1500 kW and wind turbine III has rated capacity of 850 kW. A power output capacity of 10 kW is regarded as one unit, so that the Wind Turbine II can be viewed as consisting of 150 such units with an equivalent installed cost of \$13,333/10 kW capacity, while Wind turbine III of 85 units at installed cost of \$25,000/10 kW capacity (assumed in absence of available data). Following are the curve fitted equations obtained from the data presented on the manufacturer's website. The equations are employed to analyze wind energy available for each selected city:

### **I Model for Wind Turbine-I of Small Capacity (10 kW)**

$$W_p = 0 \text{ for } V_w \leq 3.0 \text{ and } V_w \geq 24.0 \text{ m/s} \quad 4.12$$

For  $V_w > 3.0$  and  $V_w \leq 19.0$  m/s

$$W_p = -15.3057 + 1.36437 V_w - 4.0433 \times 10^{-9} \exp(V_w) + 255.7983 / V_w^{1.5} - 342.0495 / V_w^2 \quad 4.13$$

For  $V_w > 19.0$  and  $V_w \leq 24.0$  m/s

$$W_p = 14.480725 - 0.00030926 V_w^3 \quad 4.14$$

### **II Model for Wind Turbine –II of High Capacity (1500 kW)**

For  $3.0 < V_w < 8.0$  m/s

$$W_p = 90.80186 + 6.0286 V_w^{2.5} - 73.4653 V_w^{0.5} \ln(V_w) \quad 4.15$$

For  $8.0 < V_w < 10.5$  m/s

$$W_p = 1.0 / (0.000758213 - 2.5284 \times 10^{-9} \exp(V_w) + 1.737485522 \exp(-V_w)) \quad 4.16$$

For  $10.5 < V_w < 12.0$  m/s

$$W_p = (1510.557 - 645.596 \ln(V_w)) / (1.0 - 0.427557 \ln(V_w)) \quad 4.17$$

For  $V_w > 12.0$  and  $V_w < 20.0$  m/s

$$W_p = 1500 \text{ kW}$$

### **III Model for Wind Turbine – III of Medium Capacity (850 kW)**

$$W_p = 0 \text{ for } V_w < 3.0 \text{ m/s or } V_w > 25.0 \text{ m/s} \quad 4.18$$

For  $3.0 < V_w < 8.0$  m/s

$$W_p = -17574.955 + 21.00166 V_w^2 \ln(V_w) + 53568.91/V_w^{0.5} - 111091.49 \ln(V_w)/(V_w)^2 \quad 4.19$$

**Table 4.3** Basic Economic Data of Wind Turbines

Wind Turbine	Rated Capacity	Capital Costs	Comments
I	10 kW	\$36,000	This is more suitable as an individual unit for a small commercial building or large residential building.
II	1500 kW	\$2,000,000 or \$13,333 per unit of 10kW capacity	This is ideally suited for a wind farm community.
III	850 kW	\$2,125,000 or \$25,000 per unit of 10 kW capacity	This is suited for a large sized independent commercial building or for families of a small neighborhood.

For  $8.0 < V_w < 11.0$  m/s

$$W_p = 504.14327 + 0.003253 \exp(V_w) - 637089.12 \exp(-V_w) \quad 4.20$$

For  $11.0 < V_w < 16.0$  m/s

$$W_p = -243.9358 + 24.4303 V_w^2 - 5.03922 V_w^{2.5} \quad 4.21$$

For  $16.0 < V_w < 25.0\text{m/s}$

$$W_p = 850 \text{ kW}$$

The total renewable power ( $W_{\text{tot, re}}$ ) produced for a given hour can be given as

$$W_{\text{tot, re}} = \sum W_{\text{pv}} N_{\text{pv}} + \sum W_{\text{wt}} N_{\text{wt}} \quad 4.22$$

where,

$W_{\text{pv}}$  = hourly power produced by the PV panel per panel, kW

$W_{\text{wt}}$  = hourly power produced by the wind turbine per unit, kW

$N_{\text{pv}}$  = number of PV panels

$N_{\text{wt}}$  = number of wind turbine units of capacity 10 kW

### 4.3 Economic Analysis

The major concern in the design of an electric power system which utilizes renewable energy sources is the accurate selection of system components that can economically satisfy the load demand.

The system's components are determined subject to:

- Minimize the cost of electricity production (\$/kWh)
- Minimize the payback period
- To ensure that the load meets the demand as per the criteria decided

The following basic equations related to economic analysis are presented here to evaluate the economic feasibility of renewable energy technologies:

Annual cost, (A) of total investment for purchase of PV panels and wind turbines is given by

$$A = P \left[ \frac{i (1+i)^n}{(1+i)^n - 1} \right] \frac{ets}{100} \quad 4.23$$

where,

ets = equivalent total subsidies that includes federal, local and other incentives

The total principal investment, P is given by

$$P = C_{pv} + C_{wt} \quad 4.24$$

The total annual kWh electrical energy ( $E_{ann,kWh}$ ) generated is given by

$$E_{ann,kWh} = (E_{ann,kWh} N_{pv} + E_{ann,wt} N_{wt}) \quad 4.25$$

The cost of electric power produced ( $C_{ep}$ ) is given by

$$C_{ep} = A / (E_{ann,kWh}) \quad 4.26$$

The annual cost of space heating ( $C_{htg}$ ) is given by

$$C_{htg} = \sum C_h W_{hl} (t) \quad 4.27$$

where,

$C_h$  = cost of heating fuel (natural gas for ZEEB), in case a heat pump is employed to heat the space (ZEB) then  $C_h$  is replaced with  $C_e$ .



$W_{hl}$  = hourly heating load at the hour, t

The total annual cost of building operations ( $C_{opr}$ ) is given by

$$C_{opr} = \sum C_e \{ W_c(t) + W_{eqm}(t) + W_{light}(t) + W_{aux}(t) \} + C_{htg} \quad 4.28$$

The simple payback period (PB) for ZEEB is given by

$$PB = \frac{P (ets/100)}{(C_{opr} - C_{htg})} \quad 4.29$$

The simple payback period (PB) for ZEB is given by

$$PB = \frac{P (ets/100)}{C_{opr}} \quad 4.30$$

### **Evaluation of Photovoltaic (PV) System with TABLET Code**

The characteristics of PV panels described earlier are included in the TABLET code. This code is a comprehensive program developed based on the Transfer Function Method (TFM) that evaluates the hourly building loads, the HVAC equipment loads, monthly and annual operational costs. It also evaluates the impact of energy efficiency technologies on the building operational costs. The details on the method by which the program evaluates the transient building loads due to solar energy and other loads are presented in the Appendix.

Building loads are evaluated at every hour using the TMY3 hourly weather data developed by NREL inputted into the TABLET code. This software also evaluates the number of PV panels and wind turbines required to reach the status of zero electrical

energy cost building (ZEEB) or zero energy cost building (ZEB). The ZEEB employs natural gas heater to meet the space heat loads during the winter, while ZEB employs a heat pump.

The electric power produced by the PV panel system rarely equals to the electric power demand by the building system for a given hour. If it produces more, it feeds the excess power to the connected grid; otherwise it will draw the deficit power from the grid. The computer code adjusts the actual power interactions after taking into account the efficiency of the invertors and other conditioning modules.

### **Procedure to Perform Computer Simulations Using TABLET Code**

- In order to download the weather data into the code for the city in which the building is located for determination of building loads, the city is selected as shown in the Figure 4.3. For example, the city of Chattanooga, TN is selected as shown below.

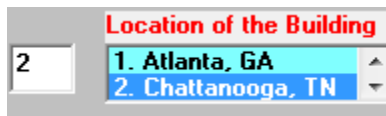


**Figure 4.3** Selection of location

- The selection of roof, wall and floor material is done for the selected city in above step. The code contains the data for forty two different types of walls and roofs materials. When they are selected, the program downloads the transfer function conduction coefficients as well as the overall heat transfer coefficients for the chosen roof or wall. For the building under consideration, roof is considered to be of “4 inch h.w. deck w/4.54 inch insulation and 2 inch h.w RTS” and walls to be of “face brick and 8 inch l.w.

concrete with 5 inch insulation” facing all directions. As described earlier, windows area is already selected, but can be changed as per the user’s needs and building construction.

	Wall Details			Window Glass Details		
	Construction Type	U-Factor (Btu/hr/ft <sup>2</sup> .F)	Area (ft <sup>2</sup> )	Area (ft <sup>2</sup> )	U-Factor (Btu/hr/ft <sup>2</sup> .F)	Shade Coef
Roof	19. 4 in. h.w. deck w/4.54 in. ins. and 2 in. h.w. RTS 20. 1.36 in. insulation with 8 in. l.w. concrete deck	0.059	10000	0	0.8	0.85
E. Wall	39. Face brick and 8 in. l.w. concrete with 5 in. insul. 40. Face brick, 12 in. h.w. block(fld), 6in. insul	0.04	1000	0	0.8	0.85
S. Wall	38. 6 in. ins. w/12 in. h.w. block(fld) and face brick 39. Face brick and 8 in. l.w. concrete with 5 in. insul.	0.04	900	100	0.8	0.85
W. Wall	38. 6 in. ins. w/12 in. h.w. block(fld) and face brick 39. Face brick and 8 in. l.w. concrete with 5 in. insul.	0.04	1000	0	0.8	0.85
N. Wall	38. 6 in. ins. w/12 in. h.w. block(fld) and face brick 39. Face brick and 8 in. l.w. concrete with 5 in. insul.	0.04	900	100	0.8	0.85
Floor	18. 2 in. h.w. conc. dk w/6 in. ins. and 2 in. h.w. RTS 19. 4 in. h.w. deck w/4.54 in. ins. and 2 in. h.w. RTS	0.059	10000	0	0.8	0.85
NE. Wall	1. Steel siding with 4 in. insulation 2. Frame wall with 5 in. insulation		0	0	0.8	0.85
SE. Wall	1. Steel siding with 4 in. insulation 2. Frame wall with 5 in. insulation		0	0	0.8	0.85
SW. Wall	1. Steel siding with 4 in. insulation 2. Frame wall with 5 in. insulation		0	0	0.8	0.85
NW. Wall	1. Steel siding with 4 in. insulation 2. Frame wall with 5 in. insulation		0	0	0.8	0.85

**Figure 4.4** Selection of Building Envelope Type

If the walls facing NE, SE, NW, SW directions have significant areas, then they are chosen too. The other HVAC related input data such as ventilation rates, air infiltration, hot water requirements, floor height, night thermostat setback settings for winter and summer, energy efficiency measures such as use of economizer, energy recovery device, demand controlled ventilation, dedicated outside air system are chosen if required. For this study, such energy efficiency improvement measures have not been considered.

The option of using the renewable energy resources, such as PV panels or/and wind turbines along with their corresponding related data can be chosen before the calculations are begun by the code.

The code will estimate the heating and cooling loads, equipment loads, and energy costs, after the buttons shown below were clicked by the user of the program, successively.



The estimated peak heating and cooling loads along with the time of occurrence for these loads are shown in the Figure 4.5.

	P. Loads (Tons)				
	latent	total	Month	Day	Time
Heating	2.4	-10.3	12	20	8
Cooling	3.9	14.5	6	28	16

**Figure 4.5** Peak Building Loads

The window at the bottom right corner of the monitor screen shows the total annual operating costs of the building. If no renewable energy resources option is chosen before the computer run, then the total annual operating cost shown in this window would be that of a conventional system. This data of the conventional operating cost is to be inserted in the alternate cost of operation window, before the program is run again with the option of renewable energy resources to estimate the simple payback period. As seen in Figure 4.6 seven possible renewable energy system configurations with or without grid connection are given. By inserting a corresponding number in the window box next to it will allow the code to simulate that particular system.



**Figure 4.6** System selection

The white window boxes shown on the computer monitor screen contains the output data generated by the code, while the blue/gray ones contain the input data inserted by the user.

### Optimizing PV Panels to Meet the Demand Load

An initial default number 400 for PV panels considered to meet the demand load.

For a system that uses only the PV panels and not the hybrid system, the default number of panels of 400 in the window can be varied iteratively, until the total annual operating cost is close to zero for a zero-energy building.

PV System					Utility P. Price	Total (kWh)
	No Panels	Mode of Oper	Cost, \$/W	Factor		Production / yr
<input type="radio"/> Off	400	1	2.7	2		110344.3 PV
<input checked="" type="radio"/> On						
Simple Payback (yrs)	16.3					
A. Cost of Operation				12560		
						0 Wind

**Figure 4.7** Calculation for Required Number of PV panel

In TABLET, the PV panel considered for analysis and its basic economic data are shown in Table 4.4. The cost of the PV panels can be changed by the user to analyze different PV panels available in the market.

**Table 4.4** Basic Economic Data of PV panels

Component	Rated Capacity	Capital Costs	Comments
PV Panel	220 Watts	\$ 2.7/ panel	This price includes the cost of inverter and wiring.

It is assumed that the utility would buy back the excess electrical energy generated by a building and fed to the grid at a rate twice than what they charge to the consumer giving a UPF of 2.

*The numerical optimization is carried out by changing the required number of panels until the total annual building operation cost shown in the right bottom corner window box of the screen indicates nearly a zero value for a zero-energy cost building.*

Zero E. Bldg Based on Energy(kWh)	2181
Zero E. Bldg Based on Cost(\$/yr)	1726

**Figure 4.8** Estimation for ZEEB and ZEB

In case of a hybrid system consisting of one wind turbine, then iteration is done for the required minimum number of PV panels to reach a zero-energy cost building as it is done for a PV system alone.

For a wind turbine system alone with no PV panels attached, the above procedure can be repeated by changing the number of turbine units until the total annual building operating costs is near zero.

The results of these iterations are shown in Tables 6.1 and 6.2.

## **CHAPTER 5**

### **COMPUTATIONAL METHODOLOGY**

The building architectural, operational, utility energy costs, weather data and electrical load profiles are fed into the TABLET software, which estimates the hourly building and equipment loads along with the operational cost of the building.

The software estimates the hourly power produced by PV panels, and wind turbine units for a given hour, evaluating whether the power is drawn from the grid or fed to the grid.

The Equations (4.1-4.10) are employed in estimating the power from the PV panels and number of PV panels needed in series and parallel, while Equations (4.11-4.22) are used for wind power at a given hour. For ZEEB applications, the gas consumption is estimated by dividing the hourly heat supply rates to the space with the efficiency of the air-furnace. Finally, the Equations (4.22-4.29) are employed in making the economic evaluations. The flow-chart shown on next page represents the order of computations for this investigation.

It may be noted that the computational procedure first reads the architectural, operational, energy cost, and meteorological data from which it evaluates the various solar angles to estimate building loads, the available electrical power from the PV panels along with the power from the wind turbines for each hour for given size of PV panels and wind turbines. The code then iterates for various sizes of PV panels and wind turbines until the annual costs of operation or cost of electric power produced is minimized.



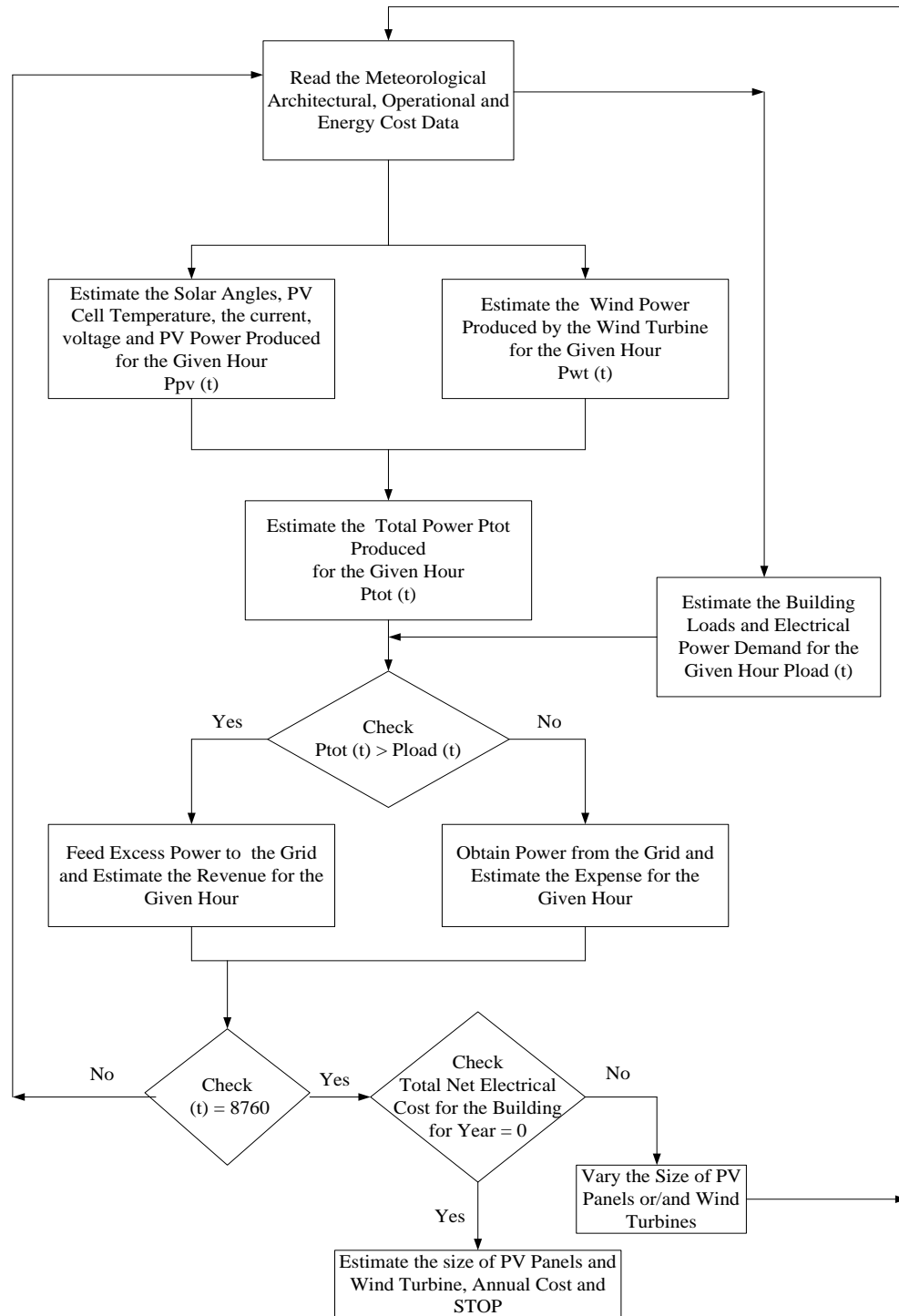


**Figure 5.1** Computation methodology of TABLET

## CHAPTER 6

### RESULTS

The results obtained from detailed computer simulations for several geographical locations are listed in the Table 6.1 and Table 6.2 and in Figures (6.1-6.16). The results shown in Table 6.1 refers to the ZEEB building that is heated by use of natural gas, while Table 6.2 represents the results of the ZEB building that is heated by use of a heat pump. The existing energy costs as charged by the local utilities are as shown in column 2 of these tables. It is assumed that the demand charge is uniform at \$ 14.5/kW for every excess kW of electric power demand above the demand limit of 50 kW, natural gas cost of \$ 1.23 per therm (100,00 Btus or 29.3 kWh) also assumed to be same for all the cities considered. The peak electrical power demand occurring in various cities are shown in column 5 of these tables. The peak demands are higher for ZEB as shown in Table 6.2 compared to the similar values in column 5 of Table 6.1, pertaining to the case of ZEEB. The values in column 6 are the AC power produced by a single PV panel that assumes an inverter efficiency of 0.94, while those in column 8 are the operating energy costs of the building without the use of any renewable energy resources.

The three (3) rows of data presented in column 7 in Tables 6.1 and 6.2 for each city considered are the annual electrical energy produced by use of Wind Turbines I, II and III, respectively of one unit of 10 kW power capacity.

The six (6) rows of data for each city presented in column 11 in Tables 6.1 and 6.2 refer to the following cases:

1. PV system only indicating the minimum number of PV panels required to meet ZEEB (Table 6.1) and ZEB (Table 6.2)
2. A hybrid system of PV and one Wind Turbine I unit indicating the minimum number of PV panels plus one unit of Wind turbine I required to meet ZEEB (Table 6.1) and ZEB (Table 6.2).
3. A hybrid system of PV and one Wind Turbine II unit indicating the minimum number of PV panels plus one unit of Wind turbine II required to meet ZEEB (Table 6.1) and ZEB (Table 6.2).
4. A hybrid system of PV and one Wind Turbine III unit indicating the minimum number of PV panels plus one unit of Wind turbine III required to meet ZEEB (Table 6.1) and ZEB (Table 6.2).
5. A hybrid system of PV and several units of Wind Turbine II indicating the minimum number of PV panels Wind turbine II units required to meet ZEEB (Table 6.1) and ZEB (Table 6.2).
6. Wind power system only consisting of several units of Wind Turbine II indicating the minimum number of Wind turbine II units required to meet ZEEB (Table 6.1) and ZEB (Table 6.2).

The six (6) rows of data for each city in columns 10 through 14 as presented in Tables 6.1 and 6.2 refers to the above six cases.

The negative values for cost of electricity generated as shown in column 14 of Tables 6.1 and 6.2 implies that the user of the renewable energy resources for these cities with the existing values of utility energy costs will derive revenue from generation of electric power as the utility would buy the excess electric power generated and fed to the

grid at an assumed cost, which is twice the cost they normally charges as listed in column 2 of Tables 6.1 and 6.2.

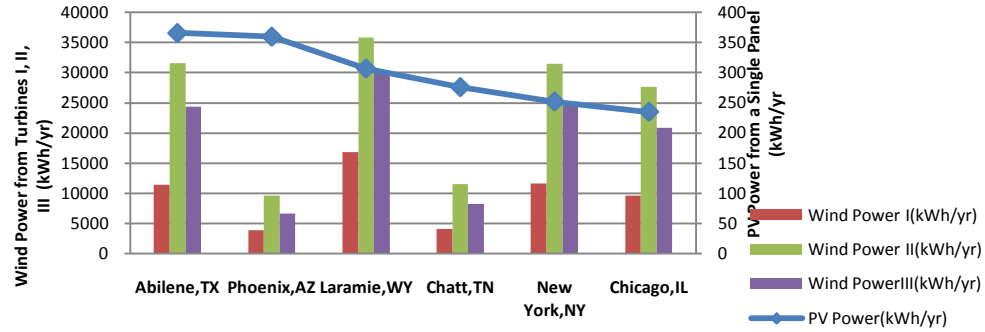


**Figure 6.1** Variation of PV and Wind Power for Various Cities

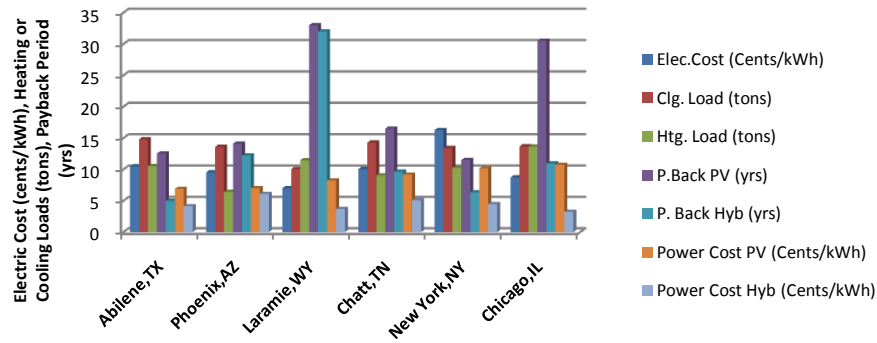


**Figure 6.2** Variation of Electric Power Cost, Heating, Cooling Load, and Payback Period for Various Cities in US for Zero-Electrical Energy Building

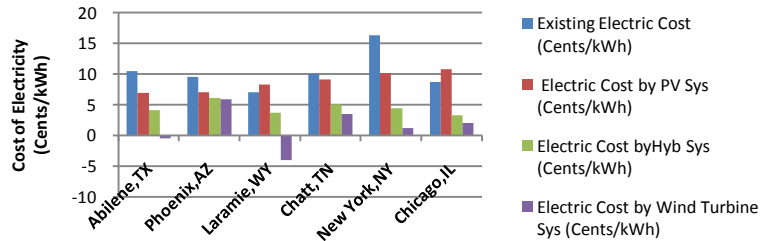


**Figure 6.3** Variation of Electric Power Cost for Various Cities in US for Zero-Electrical Energy Building

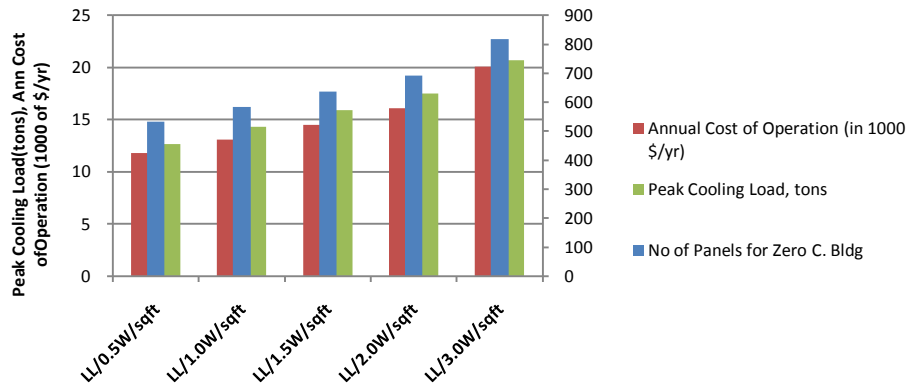


**Figure 6.4** Variation of Cooling load, Annual Cost of Operation and Number of PV Panels Required with Lighting Load for Various Cities in US for Zero Energy Cost Building

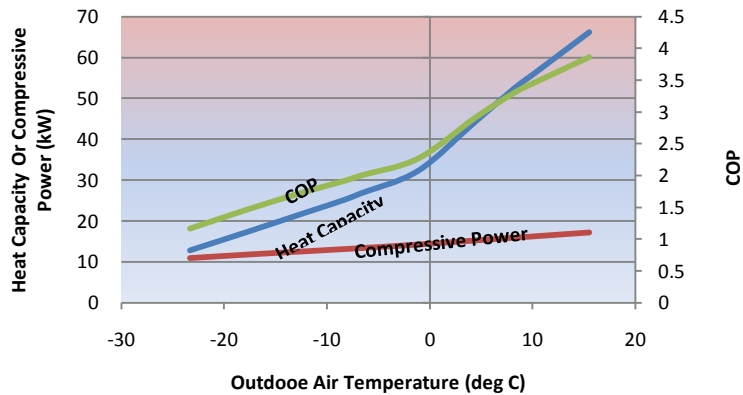


**Figure 6.5** Variation of COP, Heating Capacity and Compressive Power with Temperature of Outside Air

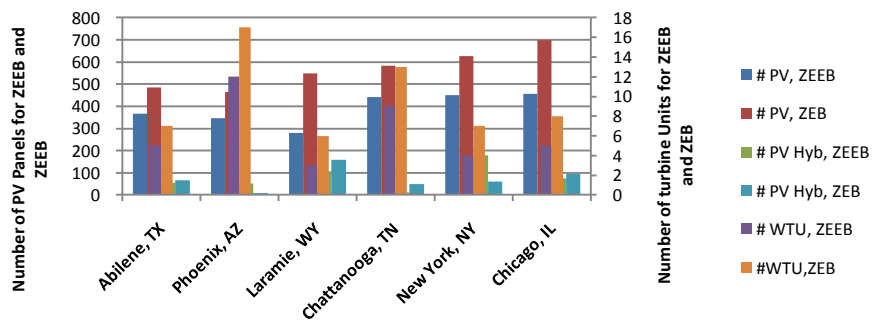


**Figure 6.6** Variation of Number of PV Panels and Wind Turbine Units for Various Cities in US for ZEEB and ZEB

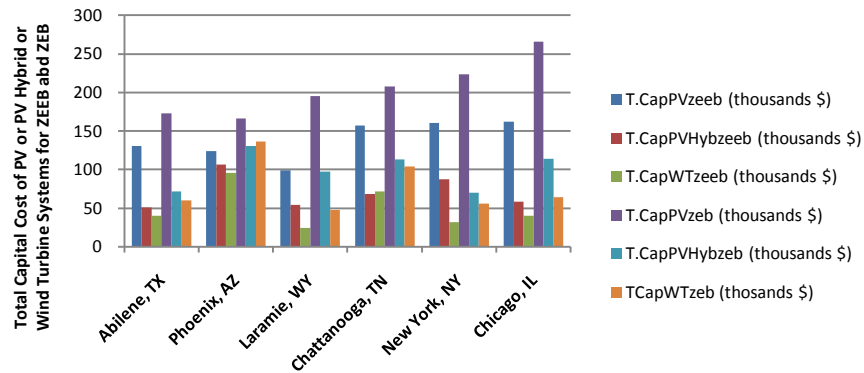


**Figure 6.7** Variation of Total Capital Cost of PV, Hybrid and Wind Turbine Units for Various Cities in US for ZEEB and ZEB

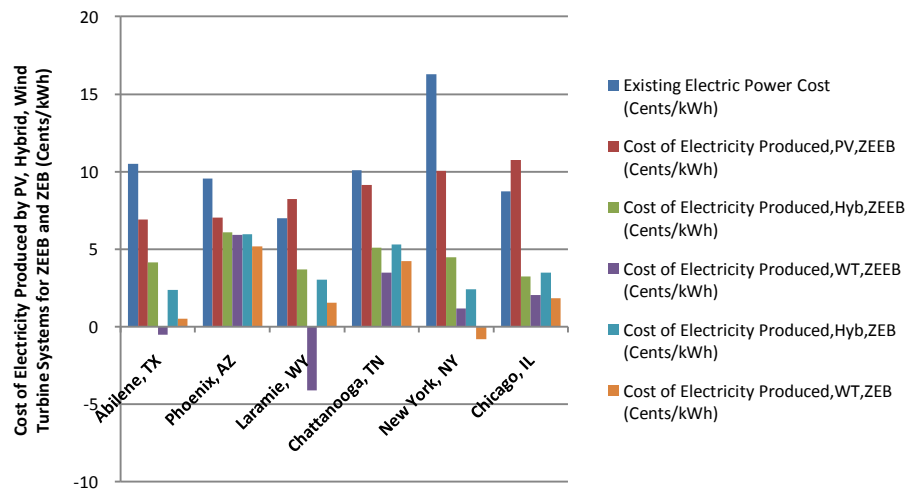


**Figure 6.8** Variation of Cost of Electricity produced from PV, Hybrid and Wind Turbine Units for Various Cities in US for ZEEB and ZEB

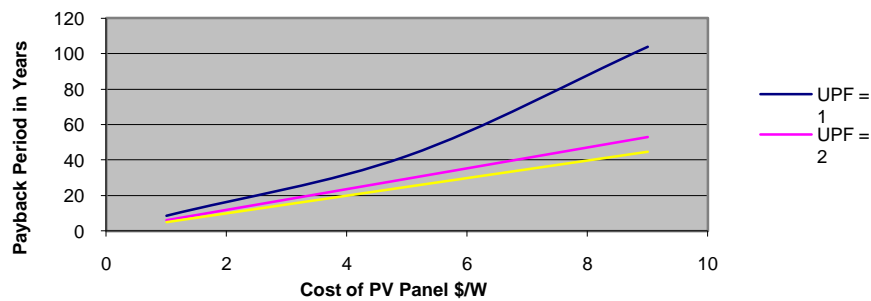


**Figure 6.9** Variation of Payback Period with PV Cost and Utility Payback Factor (UPF)

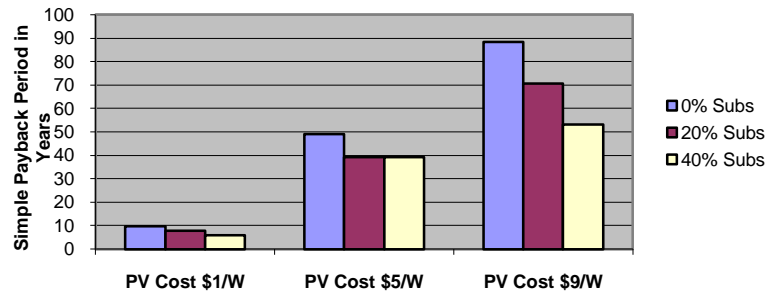


**Figure 6.10** Variation of Payback Period with Cost of PV Panels and Rate of Subsidies

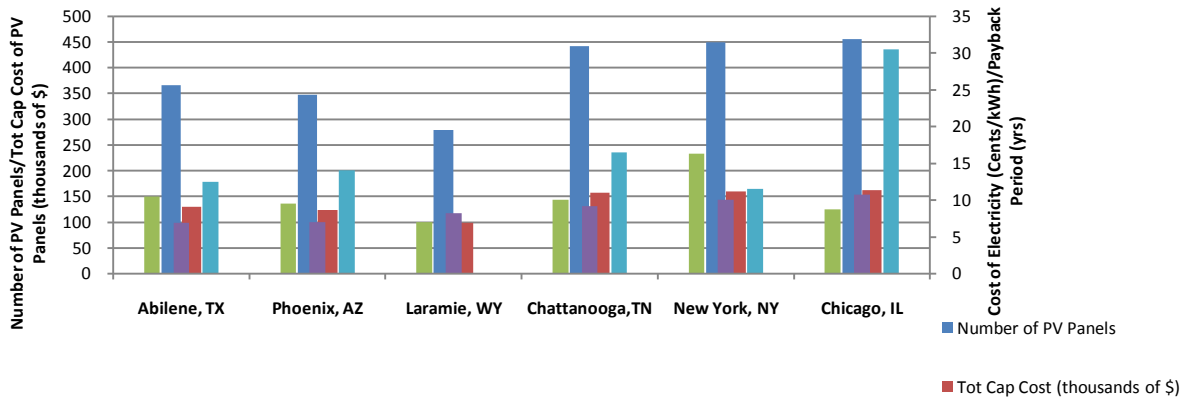


**Figure 6.11** Variations of PV Panels, Capital Cost. Electricity Cost and Payback Period for Various Cities in US for Zero-Electric Energy Building

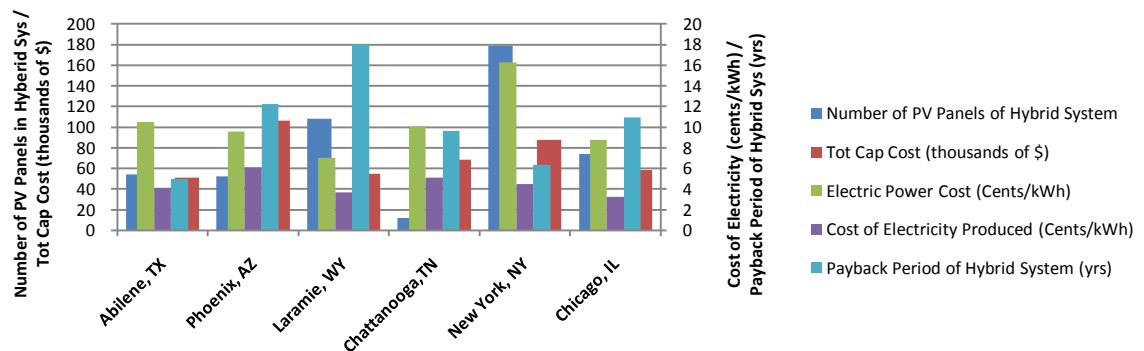


**Figure 6.12** Variations of PV Panels, Capital Cost. Electricity Cost and Payback Period of Hybrid System for Various Cities in US for Zero-Electric Energy Building

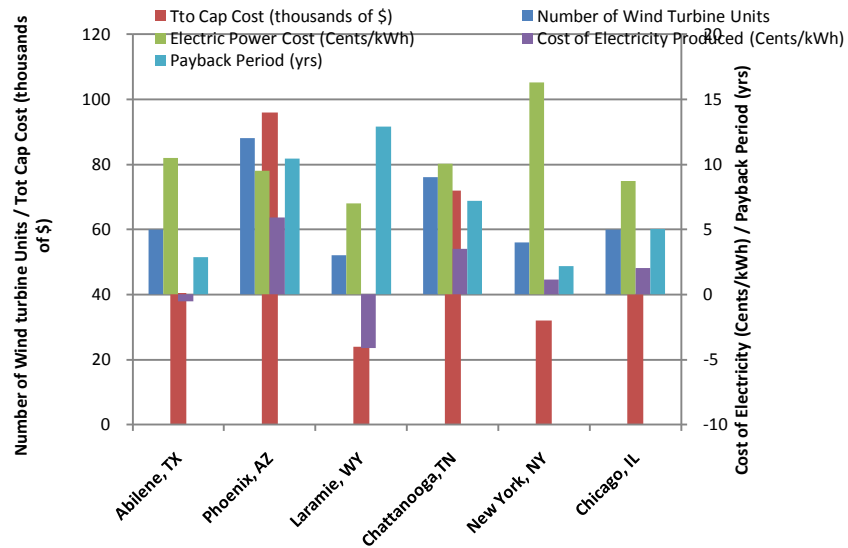


**Figure 6.13** Variations of Wind Turbine Units, Capital Cost, Electricity Cost and Payback Period of Wind Power System for Various Cities in US for Zero-Electric Energy Building

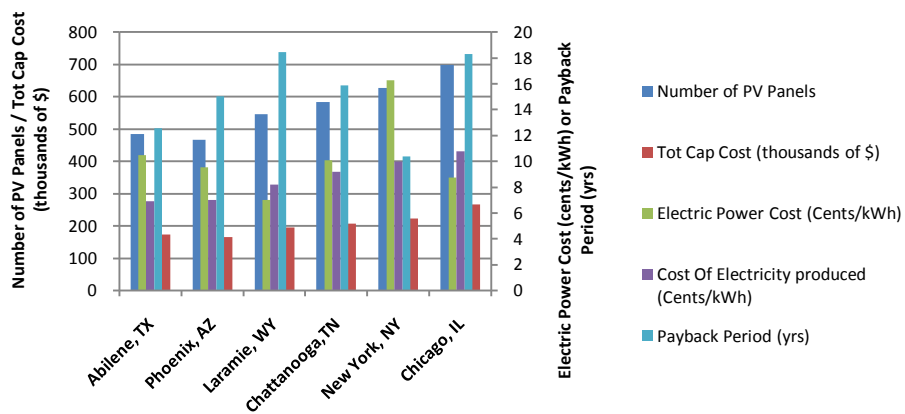


**Figure 6.14** Variations of PV Panels, Capital Cost, Electricity Cost and Payback Period for Various Cities in US for Zero Energy Building



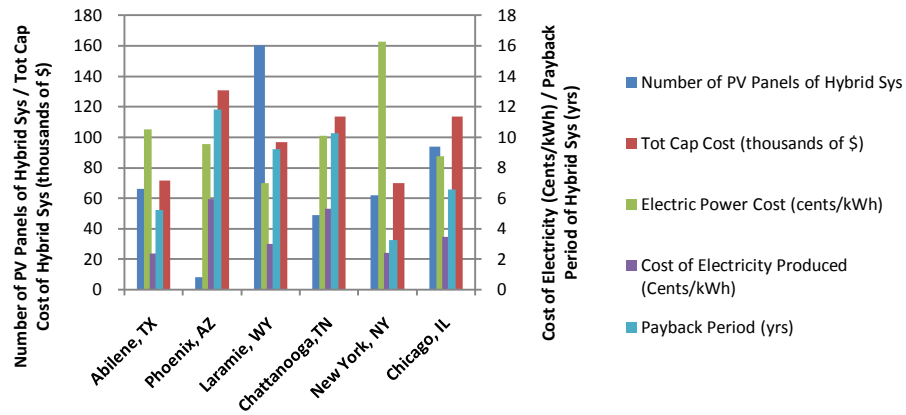


**Figure 6.15** Variations of PV Panels, Capital Cost, Electricity Cost and Payback Period of Hybrid System for Various Cities in US for Zero Energy Building

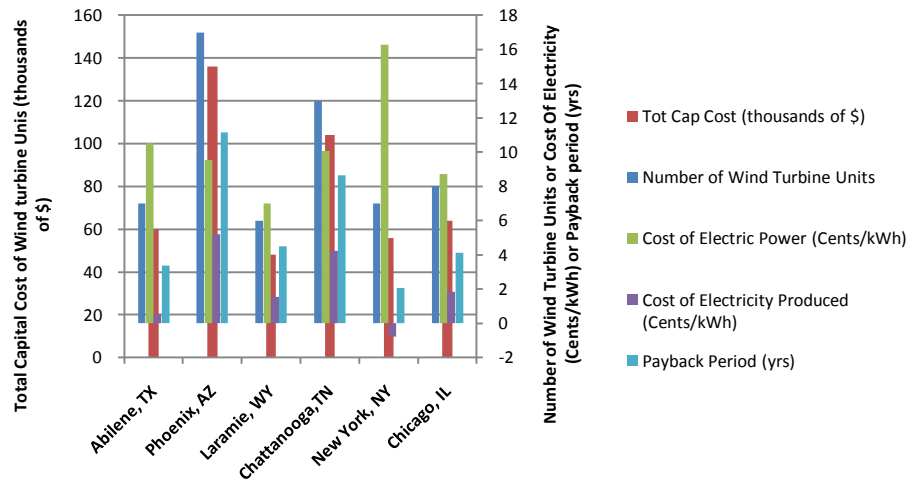


**Figure 6.16** Variations of Wind Turbine Units, Capital Cost, Electricity Cost and Payback Period of Wind Power System for Various Cities in US for Zero Energy Building

**Table 6.1** Evaluation of Zero-Electrical Energy Building with Hybrid PV Panel and Wind Turbine Systems for Various U.S Cities

City 1	E. Pow Cost C/kWh 2	P. Clg Load tons 3	P.Htg Load tons 4	Peak Elec Load (kW) 5	Ann. PV E. Energy /Panel (kWh/yr) 6	Ann. E Energy By W.Tur (kWh/yr) 7	Tot. Ann Operating Cost W/O RE (\$/yr) 8	Tot. E Demand Cost (\$/yr) 9	Tot. Ann Cost PV&W.T (\$/yr) 10	No. PV Panels + W.T units (type)Req'd 11 <sup>1</sup>	S. Pay back (Yrs) 12 <sup>2</sup>	Tot Cap. Cost (thousands, \$) W/O Subs / (W. Subs) 13 <sup>3</sup>	Cost of E.Pow Prod'd C/kWh 14 <sup>4</sup>
1. Abilene, TX	10.5	14.81	10.54	46.1	366.0	- 11,404 (I) 31,627 (II) 24,382 (III)	13,416	0	1,472 1,431 1,431 1,480 1,439 1,439(-3633)	366 + 0 346 + 1 (I) 315 + 1 (II) 326 + 1 (III) 54 + 4 (III) 0 + 5 (III)	12.53 14.10 11.70 12.85 5.0 2.89	217.4 (130.4) 241.5 (144.9) 200.4 (120.3) 218.6 (131.2) 85.4 (51.2) 66.7 (40.4)	6.91 7.45 5.81 6.48 4.14 <b>-0.50</b>
2. Phoenix, AZ	9.54	13.6	6.42	45.9	360.0	- 3,932 (I) 9,579 (II) 6,687 (III)	11,787	0	749 749 733 746 769 337 (-421)	347 + 0 343 + 1 (I) 337 + 1 (II) 340 + 1 (III) 52 + 11 (II) 0 + 12 (II)	14.1 16.45 14.62 15.5 12.23 10.45	206.1 (123.7) 239.7 (143.9) 213.5 (128.1) 227.0 (136.2) 177.6 (106.5) 160.0 (96.0)	7.03 8.01 6.94 7.49 6.09 5.93
3. Laramie, WY	7.01	10.06	11.46	32.4	307.0	- 16,840 (I) 35,825 (II) 30,125 (III)	10,170	0	4,895 4,921 4,882 4,861 4,922 4,890(-6100)	279 + 0 252 + 1 (I) 218 + 1 (II) 228 + 1 (III) 108 + 2 (II) 0 + 3 (III)	264.5 306.5 223 244 149 12.91	165.7 (99.4) 185.7 (111.4) 142.8 (85.7) 160.4 (96.3) 90.8 (54.5) 40.0 (24.0)	8.24 8.39 5.92 6.82 3.69 <b>-4.09</b>
4. Chattanooga, TN	10.08	14.29	9.04	44.1	276.0	- 4,050 (I) 11,514 (II) 8,186 (III)	12,797	0	1,606 1,591 1,595 1,616 1,627 1,650(-1480)	442 + 0 436 + 1 (I) 420 + 1 (II) 427 + 1 (III) 12 + 8 (II) 0 + 9 (II)	16.51 18.51 16.45 17.5 9.66 7.22	262.6 (157.3) 295.0 (177.0) 262.8 (157.7) 278.6 (167.2) 113.8 (68.3) 120.0 (72.0)	9.16 10.10 8.78 9.41 5.08 3.5
5. New York, N.Y	16.28	13.42	10.25	44.2	252.0	- 11,652 (I) 31,468 (II) 24,569 (III)	19,069	0	2,562 2,595 2,581 2,587 2,613 2,618(-813)	450 + 0 433 + 1 (I) 390 + 1 (II) 406 + 1 (III) 179 + 3 (II) 0 + 4 (II)	11.51 12.71 10.65 11.54 6.35 2.19	267.3 (160.4) 293.2 (175.9) 245.0 (147.0) 266.2 (159.7) 146.3 (87.8) 53.3 (32.0)	10.03 10.33 8.64 8.93 4.47 1.16
6. Chicago, IL	8.74	13.69	13.64	44.9	235.0	- 9580 (I) 27,699 (II) 20,827 (III)	11,865	0	3265 3265 3242 3242 3253 677 (-2580)	456 + 0 443 + 1 (I) 405 + 1 (II) 421 + 1 (III) 74 + 4 (II) 0 + 5 (II)	30.5 33.75 28.52 30.9 10.95 5.06	270.9 (162.5) 299.1 (179.5) 253.9 (152.3) 275.1 (165.0) 97.3 (58.4) 66.7 (40.0)	10.76 11.2 8.8 9.78 3.23 2.05

The above results are for a commercial building of 10,000 sq.ft area, made of standard materials of roof and walls with 40 occupants, 10 kW of equipment load, 1 W/ft<sup>2</sup> of lighting load, 15 cfm of ventilation, 0.15 ACH of infiltration, 100 sq.ft of glass area in south, north walls with smaller loads during nights, weekend, and holidays.

1 The upper number refers to use of use of PV Panels alone required for zero energy building with zero electrical energy cost, while lower number refers to number of PV panels required plus one Wind turbine of 11.0 kW rated capacity to make zero electrical energy building.

2 The upper number refers to payback period with PV panels alone, while the lower number refers to hybrid system of PV panels plus one Wind turbine for zero electrical energy building.

3 The upper number refers to capital cost with PV panels alone, while the lower number refers to hybrid system of PV panels plus one Wind turbine with capital cost of \$ 21,600 for zero electrical energy building.

4 The upper number refers to the cost of electricity produced by use of PV panels alone; number refers to one with Wind turbine alone.

**Table 6.2** Evaluation of Zero- Energy Building with Hybrid PV Panel and Wind Turbine Systems for Various U.S Cities

City	E. Pow Cost C/kWh	P. Clg Load tons	P.Htg Load tons	Peak Elec Load (kW)	Ann. PV E. Energy /Panel (kWh/yr)	Ann. E Energy By W.Tur (kWh/yr)	Tot. Ann Operating Cost W/O RE (\$/yr)	Tot. E Demand Cost (\$/yr)	Tot. Ann Cost PV&W.T (\$/yr)	No. PV Panels + W.T units (type)Req'd 11 <sup>1</sup>	S. Pay back (Yrs)	Tot Cap. Cost (thousands, \$) W/O Subs / (W. Subs) 13 <sup>3</sup>	Cost of E.Pow Prod'd C/kWh 14 <sup>4</sup>
1	2	3	4	5	6	7	8	9	10	11 <sup>1</sup>	12 <sup>2</sup>	13 <sup>3</sup>	14 <sup>4</sup>
1. Abilene, TX	10.5	14.81	10.54	65.5	366.0	- 11,404 (I) 31,627 (II) 24,382 (III)	13,725	698 475 360 283	   <b>0</b> <b>0</b> <b>-2,820</b>	484 + 0 469+ 1(I) 445+ 1(II) 453+ 1(III) 66+ 6 (II) 0+ 7 (II)	12.57 13.77 12.12 12.85 5.21 3.38	287.5 (172.5) 314.6 (188.8) 277.7 (166.6) 294.1 (176.5) 119.2 (71.5) 93.3 (60.0)	6.91 7.3 6.1 6.6 2.37 0.52
2. Phoenix, AZ	9.54	13.6	6.42	58.2	360.0	- 3,932 (I) 9,579 (II) 6,687 (III)	11,030	389 300 268 269	   <b>0</b> <b>0</b> <b>-1,148</b>	466 + 0 461+ 1(I) 456+ 1(II) 458+ 1(III) 8 + 16 (II) 0 + 17 (II)	15.03 16.8 15.35 16.17 11.84 11.17	276.8 (166.1) 309.8 (185.9) 284.2 (170.5) 297.1 (178.2) 218.1 (130.8) 226.7 (136.0)	7.00 7.8 7.0 7.4 5.95 5.2
3. Laramie, WY	7.01	10.06	11.46	71.1	307.0	- 16,840 (I) 35,825 (II) 30,125 (III)	10,559	943 849 799 823	   <b>0</b> <b>0</b> <b>-111</b>	547 + 1 522+ 1(I) 503+ 1(II) 508+ 1(III) 160+ 5(II) 0 + 6 (II)	18.47 19.68 17.77 18.54 9.2 4.5	324.9 (195.0) 346.1 (207.6) 312.1 (187.3) 326.8 (196.1) 161.7 (97.0) 80.0 (48.0)	8.2 8.3 7.0 7.5 3.02 1.53
4. Chattanooga, TN	10.08	14.29	9.04	64.7	276.0	- 4,050 (I) 11,514 (II) 8,186 (III)	13,070	361 352 347 351	   <b>0</b> <b>0</b> <b>-1,023</b>	584 + 0 577+ 1(I) 565+ 1(II) 570+ 1(III) 49+ 12(II) 0 + 13 (II)	15.89 17.41 16.03 16.72 10.26 8.63	346.9 (208.1) 378.7 (227.2) 348.9 (209.4) 363.6 (218.2) 189.1 (113.5) 173.3 (104.0)	9.17 9.9 8.9 9.4 5.3 4.24
5. New York, N.Y	16.28	13.42	10.25	67.9	252.0	- 11,652 (I) 31,468 (II) 24,569 (III)	21,541	374 310 290 313	   <b>0</b> <b>0</b> <b>-5,715</b>	627 + 0 611+ 1(I) 585+ 1(II) 594+ 1(III) 62+ 6(II) 0 + 7 (II)	10.37 11.10 10.04 10.52 3.25 2.05	372.4 (223.5) 398.9 (239.4) 360.8 (216.5) 377.8 (226.7) 116.8 (70.1) 93.3 (56.0)	10.0 10.3 8.6 9.2 2.43 <b>-0.79</b>
6. Chicago, IL	8.74	13.69	13.64	81.7	235.0	- 9580 (I) 27,699 (II) 20,827 (III)	13,596	1,167 1,090 1,014 1,057 707 890	   <b>0</b> <b>0</b> <b>-1,959</b>	699 + 0 685+ 1(I) 658+ 1(II) 668+ 1(III) 94+ 7 (II) 0 + 8 (II)	18.33 17.60 17.80 18.60 6.59 4.11	443.1 (265.9) 470.2 (282.1) 430.9 (258.6) 448.5 (269.1) 189.6 (113.7) 106.7 (64.0)	10.8 11.0 9.5 10.1 3.48 1.85

The above results are for a commercial building of 10,000 sq.ft area, made of standard materials of roof and walls with 40 occupants, 10 kW of equipment load, 1 W/ft<sup>2</sup> of lighting load, 15 cfm of ventilation, 0.15 ACH of infiltration, 100 sq.ft of glass area in south, and north walls, with smaller loads during nights, weekend, and holidays.

1. The upper number refers to use of PV Panels alone required to zero energy building with zero electrical energy cost, while lower number refers to number of PV panels required plus one Wind turbine of 11.0 kW rated capacity to make zero electrical energy building.
2. The upper number refers to payback period with PV panels alone, while the lower number refers to hybrid system of PV panels plus one Wind turbine for zero electrical energy building.
3. The upper number refers to capital cost with PV panels alone, while the lower number refers to hybrid system of PV panels plus one Wind turbine with capital cost of \$ 21,600 for zero electrical energy building.
4. The upper number refers to the cost of electricity produced by use of PV panels alone, refers to one with Wind turbine alone.

## CHAPTER 7

### CONCLUSIONS

Based on the results obtained from computer simulations done by use of hourly meteorological weather data in TABLET, a software developed by Professor Dhamshala, the following conclusions can be made:

1. A PV solar panel having an area of  $1.625 \text{ m}^2$  and rated capacity of 220 watts has produced a maximum annual output of 366 kWh in Abilene, TX and a lowest output of 235 kWh in Chicago, IL among the six cities considered in this investigation as seen in Figure 6.1. It takes 366 of these panels with no wind turbines for a *zero-electrical energy cost building* located in Abilene, TX to provide the lowest cost of electricity produced at 6.92 cents/kWh with a payback period of 12.53 years requiring an initial capital investment of \$130,400 after 40 percent subsidies. The corresponding results for other cities are shown in Figure 6.2. For a *zero-energy cost building*, the required number of panels rises to 484 with an initial capital investment of \$172,500 after 40 percent subsidies. The payback period and the cost of electricity generated remains the same for both of these buildings. In the case of ZEB, the building is heated in winter by an heat pump whose efficiency (COP) and heat capacity drops at lower outside air temperature as seen from Figure 6.5, requiring more electrical resistance heating thereby raising the peak electrical power demand and thus requiring more panels as seen in Figures 6.6, and 6.7. The required number

of panels is little lower for Phoenix, AZ for both types of buildings with maximum number of panels required for the city of Chicago, IL as shown in Tables 6.1 and 6.2.

2. The wind turbines considered in this investigation produced a maximum annual output of (16,840), (35,825), and (30,125) kWh in Laramie, WY and a lowest output of (3,932), (9,579), and (6,687) kWh in Phoenix, AZ, for Wind Turbines I, II and III, respectively among the six cities considered in this investigation. The Wind Turbine II of rated capacity 1,500 kW is the most efficient, as seen from Figure 6.1 and is therefore considered for the cases of wind and hybrid applications. It takes three (3 of equivalent capacity 10 kW for a total of 30 kW) of these units with no PV panels for a *zero-electrical energy cost building* located in Laramie, WY to provide the lowest cost of electricity produced at -4.09 cents/kWh (negative sign implying a revenue rather than an expense) with a payback period of 12.91 years requiring an initial capital investment of \$24,000 after 40 percent subsidies. For a *zero-energy cost building*, the required number of Wind Turbine II rises to 6 with an initial capital investment of \$48,000 after 40 percent subsidies. The required number of wind turbine units, the payback period, and the cost of electricity generated are estimated to be 6, 4.5 years and 1.53 cents/kWh, respectively. The required number of Wind Turbine II units increases by 1 for New York City and by 2 for Abilene, TX with very favorable values of cost of electricity generated and payback period for both types of buildings as shown in Tables 6.1 and 6.2, especially when compared to the solar applications alone. Revenue can be produced by use of wind energy in Laramie, WY, where the cost of electricity generated is -4.09 cents/kWh.

3. The hybrid system consisting of minimum number of PV panels in combination with required number of Wind Turbine II units are considered, where the bulk of electric power is produced by wind turbine as the Wind Turbine II is capable of producing the largest kWh of electrical energy per dollar of investment than any other type of turbine and PV panel considered. The number of units of wind turbines drops by 1 for all of the hybrid systems for both types of buildings and the cost of electricity produced and payback period falls between the solar and wind modes of operation, with values close to the case of wind mode of operation. The cost of electricity generated is the lowest for ZEEB for Chicago, while it is lowest for Abilene, for ZEB case. The lowest values can be attributed to the lower number of PV panels employed in these cases as seen in Tables 6.2 and 6.2.
4. The overall economics indicated by the cost of electricity generated, the payback period, the required number of PV panels or/and the wind turbine units, and the capital investment are sensitive not only to the weather data of the city, the building load components such as the number of occupants, equipment loads, lighting load, the window area, the air infiltration and ventilation rates, the existing power costs of the local utility, but the factors such as the cost of PV panel, wind turbine, the level of subsidies and the utility payback factor for power have very strong impact on the overall economics of the renewable energy as shown in Figures presented in the previous chapter.





## References

- [1] Energy Information Administration (EIA), International Energy Annual 2005 (June-October 2007),  
  
[www.eia.doe.gov/iea](http://www.eia.doe.gov/iea)
- [2] United States Environmental Protection Agency, [www.epa.gov](http://www.epa.gov)
- [3] “Renewable Energy” Godfrey Boyle second edition (2008)
- [4] Borowy BS, Salameh ZM, “Methodology for optimally sizing the combination of a battery bank and PV array in a wind/PV hybrid system, IEEE Transactions on Energy Conversion 1996; 11(2), 367-75
- [5] E.S. Gavanidou and A.G. Bakirtzis, “Design of a standalone system with renewable energy sources using trade off methods”, IEEE Trans, Energy Conversion, (1992) 42-48
- [6] J. Castle, J. Kallis, S. Moite and N. Marshall, “Analysis of merits of hybrid wind/photovoltaic concept for standalone systems”, Proc. 15<sup>th</sup> IEEE PV Specialist Conference, 1981, PP 738-743.
- [7] R.C. Bansal, T.S. Bhatti, D.P. Kothari, “On some of the design aspects of wind energy conversion systems Energy Conversion and Management”, 43 (2002) 2175-2187
- [8] H. Ibrahim, A. Ilinca, J. Perron, “Renewable and Sustainable Energy Reviews, Energy storage systems- Characteristics and comparison”.

- [9] S. Ashok, "Optimized model for community-based hybrid energy system", Renewable energy, vol.32, No.32, pp. 1155-1164, 2007
- [10] S. Diaf, G. Notton, M. Belhamel, M. Haddadi, A. Louche, "Design and techno-economical optimization for hybrid PV/wind system under various meteorological conditions", Applied Energy 85 (2008) 968-987
- [11] S. Diaf, M. Belhamel, M. Haddadi, and A. Louch, "A Methodology for Optimal Sizing of autonomous Hybrid PV/Wind System", Energy Policy 35 (2007) 5708-5718
- [12] Ai,B., Yang. H, Shen H and Liao, X 2003, "Computer aided design of PV/Wind hybrid system," Renewable Energy 28 (2003) 1491-1512
- [13] Skoplaki, E and Palyvos, J.A 2009, "Operating temperature of photovoltaic modules: A survey of pertinent correlations," Renewable Energy 34 (2009) 23-29
- [14] The Encyclopedia of Earth, [www.eoearth.org](http://www.eoearth.org)
- [15] Fundamentals of Electrical Engineering and Electronics' by S. Chand & Co Ltd, 2008. 3. V.K Mehta and Rohit Mehta
- [16] (04/18/2010) <http://pvcldrom.pveducation.org/>
- [17] SolarGen UK, [www.solargenuk.com](http://www.solargenuk.com)
- [18] Electropaedia, [www.mpoweruk.com](http://www.mpoweruk.com)
- [19] Canadian Wind Energy Atlas, [www.windatlas.ca/en/faq.php](http://www.windatlas.ca/en/faq.php)
- [20] Weblab, [www.weblab.open.ac.uk](http://www.weblab.open.ac.uk)

- [21] Scientific Electronic Library Online, [www.scielo.cl](http://www.scielo.cl)
- [22] B.K.Hodge “Alternative energy system and application” John Wiley (2010)
- [23] Mistaya Engineering Inc., [www.mistaya.ca](http://www.mistaya.ca)
- [24] Darrieus Wind Turbine Analysis, [www.windturbine-analysis.netfirms.com](http://www.windturbine-analysis.netfirms.com)
- [25] The Solar Guide, [www.thesolarguide.com](http://www.thesolarguide.com)
- [26] GE Energy, [www.gepower.com](http://www.gepower.com)
- [27] Vestas, [www.vestas.com](http://www.vestas.com)
- [28] Bergey Wind Power, [www.bergey.com](http://www.bergey.com)
- [29] Energy Education Programs, [www.energyeducation.tx.gov](http://www.energyeducation.tx.gov)



## APPENDIX I

$$I = I_L - I_D - I_{sh} = I_L - I_o \left[ \exp \left( \frac{V + IR_s}{a} \right) - 1 \right] - \frac{V + IR_s}{R_{sh}} \quad (1)$$

$$P = I V \quad (2)$$

$$I_{sc,ref} = I_{L,ref} - I_{o,ref} \left[ \exp \left( \frac{I_{sc,ref} R_{s,ref}}{a_{ref}} \right) - 1 \right] - \frac{I_{sc,ref} R_{s,ref}}{R_{sh,ref}} \quad (3)$$

$$I_{L,ref} = I_{o,ref} \left[ \exp \left( \frac{V_{oc,ref}}{a_{ref}} \right) - 1 \right] + \frac{V_{oc,ref}}{R_{sh,ref}} \quad (4)$$

$$I_{mp,ref} = I_{L,ref} - I_{o,ref} \left[ \exp \left( \frac{V_{mp,ref} + I_{mp,ref} R_{s,ref}}{a_{ref}} \right) - 1 \right] - \frac{V_{mp,ref} + I_{mp,ref} R_{s,ref}}{R_{sh,ref}} \quad (5)$$

$$\frac{I_{mp,ref}}{V_{mp,ref}} = \frac{\frac{I_{o,ref}}{a_{ref}} \exp \left( \frac{V_{mp,ref} + I_{mp,ref} R_{s,ref}}{a_{ref}} \right) + \frac{1}{R_{sh,ref}}}{1 + \frac{I_{o,ref} R_{s,ref}}{a_{ref}} \exp \left( \frac{V_{mp,ref} + I_{mp,ref} R_{s,ref}}{a_{ref}} \right) + \frac{R_{s,ref}}{R_{sh,ref}}} \quad (6)$$

$$\frac{\partial V_{oc}}{\partial T} = \mu_{V,oc} \approx \frac{V_{oc}(T_c) - V_{oc}(T_{ref})}{T_c - T_{ref}} \quad (7)$$

$$\frac{a}{a_{ref}} = \frac{T_c}{T_{ref}} \quad (8)$$

$$I_L = \frac{S}{S_{ref}} \left[ I_{L,ref} + \mu_{I,sc} (T_c - T_{c,ref}) \right] \quad (9)$$

$$\frac{I_o}{I_{o,ref}} = \left( \frac{T_c}{T_{c,ref}} \right)^3 \exp \left( \frac{E_g}{kT} \Big|_{T_{c,ref}} - \frac{E_g}{kT} \Big|_{T_c} \right) \quad (10a)$$

$$\frac{E_g}{E_{g,ref}} = 1 - C(T - T_{ref}) \quad (10b)$$

$$\frac{R_{sh}}{R_{sh,ref}} = \frac{S_{ref}}{S} \quad (11)$$

$$R_s = R_{s,ref} \quad (12)$$

$$\frac{I_{mp}}{V_{mp}} = \frac{\frac{I_o}{a} \exp \left( \frac{V_{mp} + I_{mp} R_s}{a} \right) + \frac{1}{R_{sh}}}{1 + \frac{R_s}{R_{sh}} + \frac{I_o R_s}{a} \exp \left( \frac{V_{mp} + I_{mp} R_s}{a} \right)} \quad (13)$$

$$I_{mp} = I_L - I_o \left[ \exp \left( \frac{V_{mp} + I_{mp} R_s}{a} \right) - 1 \right] - \frac{V_{mp} + I_{mp} R_s}{R_{sh}} \quad (14)$$

$$\eta_{mp} = \frac{I_{mp} V_{mp}}{A_c G_T} \quad (15)$$

$$\eta_{mp} = \eta_{mp,ref} + \mu_{\eta,mp} (T_c - T_{c,ref}) \quad (16)$$



## Solar Energy

The earth rotates about its own axis causing day and nights and simultaneously revolving in an elliptical orbit at a mean radius of about 149.6 million kilometers around the sun causing the seasons as shown in the Figure 3. As seen from this figure, the summer solstice, the day of the longest daylight occurs about June 21, while the winter solstice, the day of the longest night occurs about December 21 for northern latitudes. The equinox characterized by a day of equal lengths of daylight and nights occurs about March 23 and September 21. Thus the amount of solar energy received by a surface on the earth varies with time during the day, as

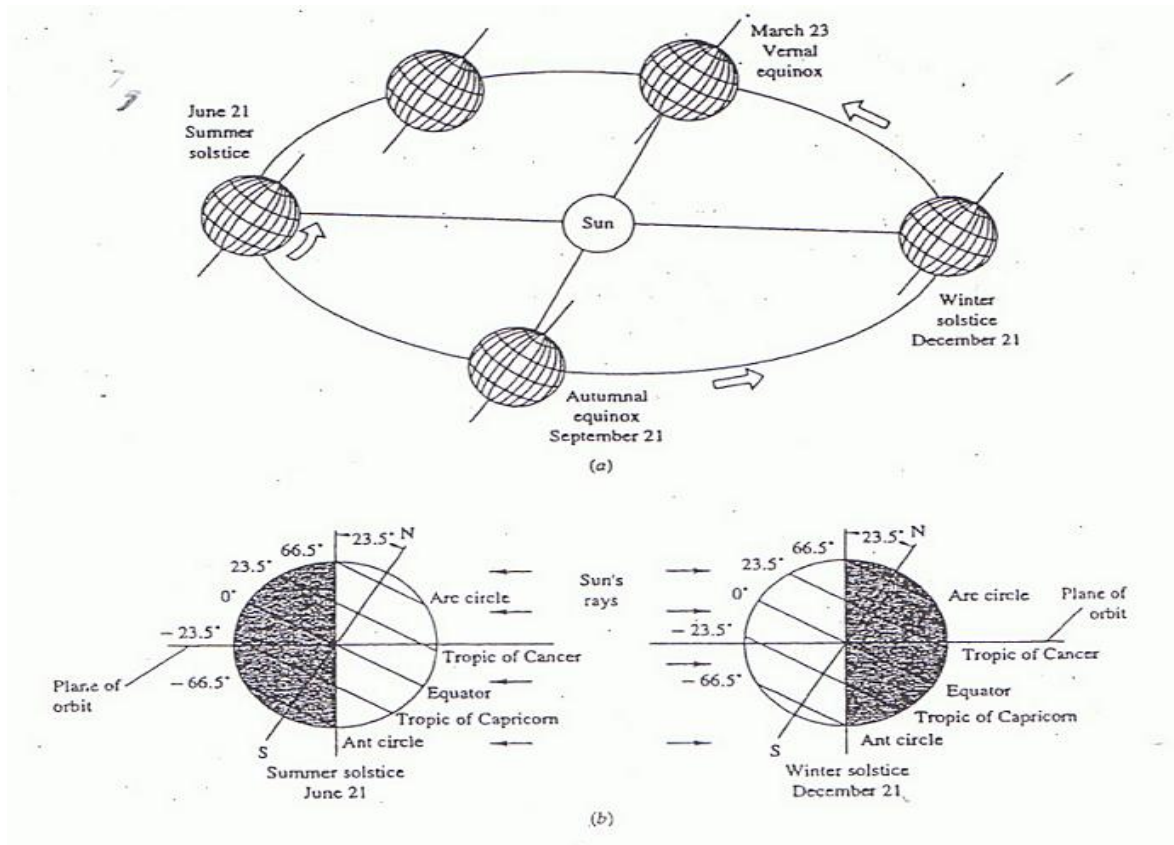


**Figure 3 Transient Nature of Solar Energy**

well as with the season and latitude of the location. The solar noon is the time of the day at which the rays from the sun are normal to the longitude of the location. The gases, dust particles and clouds present in the atmosphere scatter the *beam radiation* originating from the Sun. The scattered energy often called *diffuse energy* exists even on cloudy days. The actual energy reaching a surface on the earth is the sum of the beam (or also known as *direct radiation*) and *diffuse radiation*. The magnitude of diffuse energy reaching the surface on the earth is at the minimum on clear sky conditions, while the energy is 100 percent diffuse on a day of fully cloudy conditions.

The average rate of solar energy also known as *extra terrestrial irradiance* or *insolation* striking a surface directed normal to the solar beam outside the earth's atmosphere is termed as *Solar Constant* and its value is given as 1373 W/m<sup>2</sup> or 435.2 Bu/hr.ft<sup>2</sup>. The extra terrestrial irradiance is all beam radiation. However, due to slight eccentricity in the earth's orbit, the actual value of extra terrestrial irradiance is related as

$$I_o \left( \frac{Btu}{hr \cdot ft^2} \right) = 435.2 \left[ 1 + 0.033 \cos \left( \frac{360^\circ n}{365.25} \right) \right] \quad (1)$$

$$I_o \left( \frac{W}{m^2} \right) = 1373 \left[ 1 + 0.033 \cos \left( \frac{360^\circ n}{365.25} \right) \right] \quad (2)$$

where, n is the day of the year (= 1 for January 1).

*Estimation of Total Incident Solar Irradiance on a Surface on the Earth*

Due to the rotation of the earth about its own axis as well around the Sun, the estimate of incident solar irradiance,  $I_t$  consisting of beam and diffuse components involves determining various solar angles, namely:

Declination angle ( $\delta$ ) is the angle made by the equator with sun's rays as shown in

Figure 4b

Surface latitude angle ( $\lambda$ ) is the angle between the radius vector of the location from the center of the earth and the equatorial plane indicated in the Figure 4a

Hour angle ( $\omega$ ) is the angle between the meridian plane of the sun's rays with the local meridian at the center of the earth in an equatorial plane as shown in Figure 4a

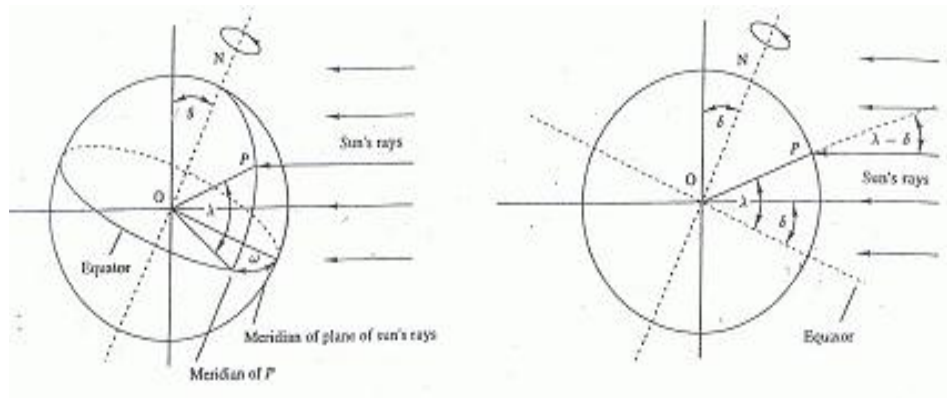
Solar azimuth angle ( $\Phi_s$ ) is the angle between the projection of the sun's rays on a local horizontal plane and the south direction as shown in Figure 5a

Solar zenith angle ( $\theta_s$ ) is the angle between the sun's rays and the normal on the local horizontal plane as shown in Figure 5a

Surface azimuth angle ( $\Phi_p$ ) is the angle between the normal to the surface with the south direction as shown in Figure 5b

Surface tilt angle ( $\theta_p$ ) is the angle between the surface and the local horizontal as shown in Figure 5b

Solar incident angle ( $\theta_i$ ) is the angle between the normal to the surface with sun's rays as shown in Figure 5b



(a) Three-Dimensional View

(b) Cross-Sectional View at Solar Noon

**Figure 4** Illustration of Latitude, hour angle and solar declination

The declination angle ( $\delta$ ) can be given as,

$$\sin \delta = -\sin 23.45^\circ \cos \frac{360^\circ (n + 10)}{365.25} \quad (3)$$

where,  $n$  is the day of the year with January 1 being  $n = 1$ .

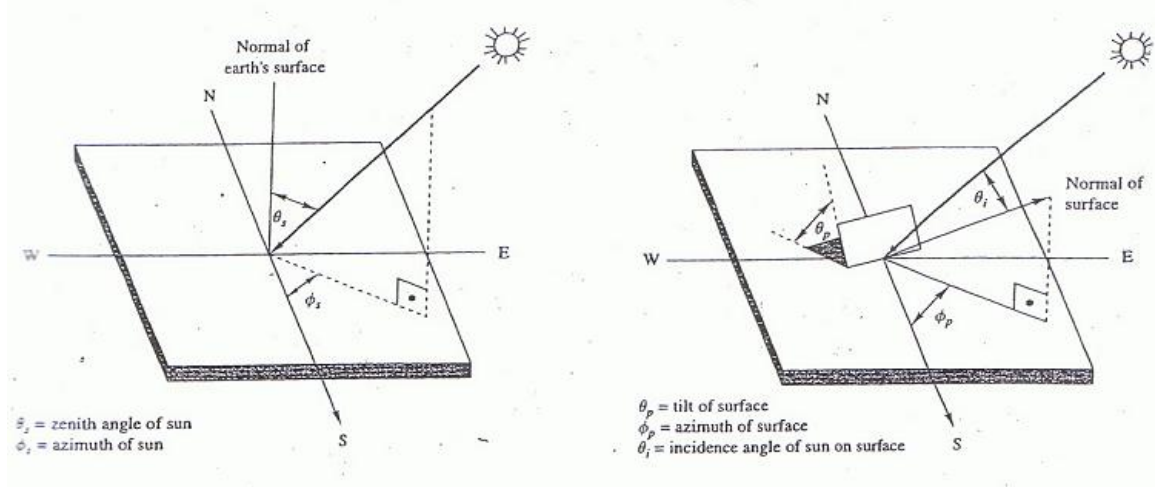


**Figure 5.** Solar Angles for a Tilted Surface

The hour angle ( $\omega$ ) can be estimated in terms of solar time ( $t_{sol}$ ) from,

$$\omega = \frac{360^0 (t_{sol} - 12h)}{24h} \quad (4)$$

The solar time,  $t_{sol}$  is related to the local standard time,  $t_{std}$  as

$$t_{sol} = t_{std} + \frac{L_{std} - L_{loc}}{15^0 / hr} + \frac{E_t}{60 \text{ min} / hr} \quad (5)$$

where  $t_{std}$  = local standard time

$L_{std}$  = longitude of the standard time, for United States, Eastern =  $75^0$ , Central =  $90^0$ ,

Mountain =  $105^0$ , Pacific =  $120^0$ .

$L_{loc}$  = longitude of the location in degrees.

$E_t$  = equation of time is the difference between the solar noon and noon time based on local Time and it varies over the year.

It may be noted that solar noon refers to the time when sun reaches the highest point in the sky. The equation of time  $E_t$  is obtained from

$$E_t = 9.87 \sin\left(\frac{360^0 (n-81)}{364}\right) - 7.53 \cos\left(\frac{360^0 (n-81)}{364}\right) - 1.5 \sin\left(\frac{360^0 (n-81)}{364}\right) \quad (6)$$

The solar zenith angle ( $\theta_s$ ) as shown in the Figure 6 can be estimated from,

$$\cos \theta_s = \cos \lambda \cos \delta \cos \omega + \sin \lambda \sin \delta \quad (7)$$

Now, the solar azimuth angle ( $\phi_s$ ) in terms of solar zenith angle ( $\theta_s$ ) is obtained as follows

$$\phi_s = \frac{\cos \delta \sin \omega}{\sin \theta_s} \quad (8)$$

Finally, the solar incident angle ( $\theta_i$ ) is given by

$$\cos \theta_i = \sin \theta_s \sin \theta_p \cos (\phi_s - \phi_p) + \cos \theta_s \cos \theta_p \quad (9)$$

where,  $\phi_s$  is the solar azimuth angle given by Equation (8) while the surface azimuth angle  $\phi_p$  as shown in the Figure 4 is the angle made by the surface normal with the south direction. The tilt angle of the surface  $\theta_p$  is the angle of inclination of the surface with local horizontal surface as shown in Figure 5.

Now the total incident solar load  $I_t$  is the sum of

- (i) the solar direct radiation ( $I_{dir}$ ) incident normal to the surface
- (ii) the solar diffuse radiation ( $I_{dif}$ ), the diffuse radiation is the radiation scattered from the surroundings and the dust particles present in the atmosphere.
- (iii) the solar radiation reflected from the ground

$$I_t = I_{dir} \cos \theta_i + I_{dif,hor} \frac{1 + \cos \theta_p}{2} + I_{glo,hor} \rho_g \frac{1 - \cos \theta_p}{2} \quad (10)$$

where,  $I_{glo,hor}$  is the global horizontal radiation incident on the horizontal surface.

The weather stations in various major cities record hourly data consisting of  $I_{dir}$ ,  $I_{dif,hor}$ ,  $I_{glo,hor}$ , the ambient air temperature, the dew point temperature, the relative humidity, wind speed and direction, cloud cover factor and many other data. The meteorologists obtained the average of 25 to 30 years of such data and designated these data as the typical meteorological year (TMY) for that city. Use of such data allows a more detailed and accurate estimate of solar loads.

### ***Estimation of Solar Irradiance from Approximate Models***

The meteorological data are being collected for various major towns in the United States and around the world. The collection of such data grew rapidly for many other towns, when the fuel cost escalated during the mid 70's. In locations where such data are not measured, attempts have been made to estimate the solar data from approximate models related to extra terrestrial solar irradiance and variables such as percentage of



sunshine or clearness index, and visibility. The following equations outline such procedures.

$$\frac{I_{dif}}{I_{glo}} = \begin{cases} 1 - 0.09 K_T & K_T \leq 0.22 \\ 0.9511 - 0.1604 K_T + 4.388 K_T^2 - 16.638 K_T^3 + 12.336 K_T^4 & 0.22 < K_T \leq 0.8 \\ 0.165 & K_T > 0.8 \end{cases} \quad (11)$$

where  $K_T$  = hourly clearness index =  $I_{glo} / I_o \cos \theta_s$

#### *Clear-Day Model*

The direct or beam diffusion,  $I_{dir}$  during a clear sky radiation is given by

$$I_{dir} = I_o \left[ a_o + a_1 \exp \left( -\frac{k}{\cos \theta_s} \right) \right] \quad (12)$$

where  $a_o$  ,  $a_1$  and  $k$  are constants as listed in Table 1.

The constants  $a_o$  ,  $a_1$  and  $k$  are dependent upon the visibility, the altitude and latitude of the location as seen from the Table 1

The diffuse irradiance  $I_{dif,hor}$  is obtained from

$$I_{dif,hor} = ( 0.271 I_o - 0.2939 I_{dir} ) \quad (13)$$

### ***Solar Heat Gain Factors***

The energy interaction across a glass window of a building consists of reflection, absorption, and transmission of incoming solar energy and reflected energy from the ground, as well as heat conduction due to temperature difference between the outside and

**Table 1 Coefficients of Clear-Day Model [72]**

(a) The coefficients  $a_o$ ,  $a_1$ , and  $k$  are expressed as a function of altitude,  $A$  above sea level ( in km), for two levels of visibility

	23 km (14.3 mi) visibility	5 km (3.11 mi) visibility
$a_o$	$r_o [0.4237 - 0.00821 (6.0 - A)^2]$	$r_o [0.2538 - 0.0063 (6.0 - A)^2]$
$a_1$	$r_1 [0.5055 + 0.00595 (6.5 - A)^2]$	$r_1 [0.7678 + 0.0010 (6.5 - A)^2]$
$k$	$r_k [0.2711 + 0.01858 (2.5 - A)^2]$	$r_k [0.2490 + 0.0810 (2.5 - A)^2]$

(b) The correction factors  $r_o$ ,  $r_1$ , and  $r_k$  are give as

Climate Type	$r_o$		$r_1$	$r_k$
	Visibility			
	23 km	5 km		
Tropical	0.95	0.92	0.98	1.02
Mid-latitude summer	0.97	0.96	0.99	1.02
Sub-arctic summer	0.99	0.98	0.99	1.01
Mid-latitude Winter	1.03	1.04	1.01	1.00

indoor air as shown in Figure 6.

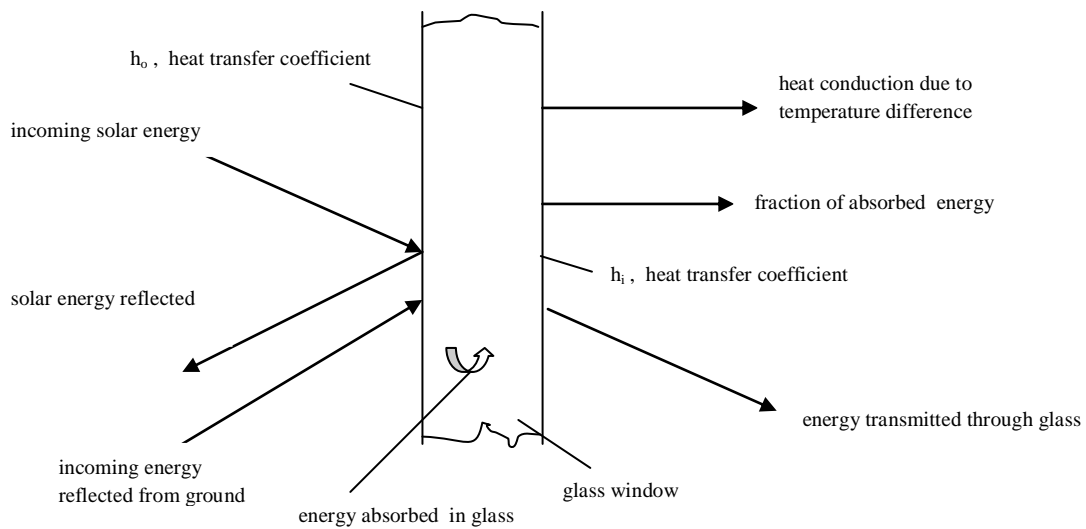


**Figure 6** Distribution of Energy Interactions Across a Glass Window

It is also indicated that a fraction of the absorbed energy in the glass is reradiated back to the indoor air.

The radiational properties of absorptivity ( $\alpha$ ) and transmittivity ( $\tau$ ) of a double-strength sheet (DSA) are often employed as a standard in determining the fractions of energy absorbed and transmitted. The actual values of the energy interactions of a given glass sheet are adjusted by multiplying the values of a DSA glass with a shading coefficient. The direct absorption ( $\alpha_D$ ) and transmission ( $\tau_D$ ) coefficients of a DSA glass are related to the incident angle  $\theta$ , and are given as

$$\alpha_D = \sum_{j=0}^5 a_j [\cos \theta]^j \quad (14a)$$

$$\tau_D = \sum_{j=0}^5 t_j [\cos \theta]^j \quad (14b)$$

The diffuse absorption ( $\alpha_d$ ) and transmission ( $\tau_d$ ) coefficients of a DSA glass are also related to the incident angle  $\theta$ , and are given as

$$\alpha_d = 2 \sum_{j=0}^5 a_j / [j + 2] \quad (15a)$$

$$\tau_d = 2 \sum_{j=0}^5 t_j / [j + 2] \quad (15b)$$

The values of coefficients  $a_j$ , and  $t_j$  are as listed in the Table 2

The direct irradiance striking the window,  $I_D$  is given as,

$$I_D = I_{dir} \cos \theta \quad \text{if } \cos \theta > 0; \text{ otherwise } I_D = 0 \quad (16)$$

The ratio, Y, of the sky diffuse irradiance to that on the horizontal surface is given as

$$Y = 0.55 + 0.437 \cos \theta + 0.313 \cos^2 \theta \quad \text{for } \cos \theta > -0.2; \quad (17)$$

otherwise  $Y = 0.45$

**Table 2** The Coefficients for DSA Glass for Calculation of Absorbance and Transmittance

j	$a_j$	$t_j$
0	0.01154	-0.00885
1	0.77674	2.71235
2	-3.94657	-0.62062
3	8.57881	7.07329
4	-8.38135	9.75995
5	3.01188	-3.89922

The diffuse radiation,  $I_{\text{dif}}$  = diffuse sky irradiance,  $I_{\text{ds}}$  + diffuse ground reflected irradiance,  $I_{\text{dg}}$

$$\text{For vertical surfaces, } I_{\text{ds}} = Y I_{\text{dif,hor}} \quad (18)$$

$$\text{For other surfaces, } I_{\text{ds}} = I_{\text{dif,hor}} (1 + \cos \theta_p) / 2 \quad (19)$$

$$\text{Diffuse ground reflected irradiance, } I_{\text{dg}} = \{I_{\text{dif,hor}} + I_{\text{dir}} \cos \theta_s\} \rho_g [1 - \cos \theta_p] / 2 \quad (20)$$

where  $\rho_g$  is the reflectance of the ground normally assumed to be 0.2.

$$\text{The transmitted component of solar energy, } I_{\text{tra}} = \tau_D I_D + 2 \tau_d [I_{\text{ds}} + I_{\text{dg}}] \quad (21)$$

$$\text{The absorbed component of solar energy, } I_{\text{abs}} = \alpha_D I_D + 2 \alpha_d [I_{\text{ds}} + I_{\text{dg}}] \quad (22)$$

The hourly solar heat gain per unit area of a DSA glass is known as *Solar Heat Gain Factor*, SHGF and is given as

$$\text{SHGF} = I_{\text{tra}} + N_i I_{\text{abs}} \quad (23)$$

where  $N_i$  represents the fraction of absorbed energy radiated back indoors and is given by

$$N_i = \frac{h_i}{h_i + h_o} \quad (24)$$

where  $h_i$  and  $h_o$  represent heat transfer coefficients at the inner and outer surfaces of the glass window, respectively.

## Evaluation of Rate of Heat Transfer Based on Transfer Function Method [72]

The following example illustrates the use of transfer function method to evaluate the rate of heat transfer from a wall exposed to the solar radiation. Consider a vertical wall, of dark color and facing west, consisting of 0.10 m (4 in) concrete with 0.05-m (2-in) insulation on the outside with sol-air temperatures as given in the second column of Table 3 for summer design conditions (July 2) for  $T_i = 25^0$  C. The transfer function coefficients for the wall as given in the ASHRAE Handbook of fundamentals [73] are as follows:

$b_0 = 0.00312$	$\sum c_n = 0.0734$	$d_0 = 1.0000$
$b_1 = 0.04173$		$d_1 = -0.94420$
$b_2 = 0.02736$		$d_2 = 0.05025$
$b_3 = 0.00119$		$d_3 = -0.00008$

The d's are dimensionless, and b's are in W/m<sup>2</sup>.K. All other coefficients are zero, and the U value is 0.693 W/m<sup>2</sup>.K

For time  $t < 0$ , it is assumed that the heat transfer to the wall  $Q_{cond, t} = 0$ .

From Equation (28) of Chapter IV,

$$\dot{Q}_{cond, t} = -\sum_{n \geq 1} d_n \dot{Q}_{cond, t-n\Delta t} + A \left( \sum_{n \geq 0} b_n T_{os, t-n\Delta t} - T_i \sum_{n \geq 0} c_n \right)$$



For unit area of the wall with area  $A = 1 \text{ m}^2$ , for the time  $t = 1 \text{ hr}$ , the above Equation reduces to

$$Q_{\text{cond}, 1} = -d_1 Q_{\text{cond}, 1-1} - d_2 Q_{\text{cond}, 1-2} - d_3 Q_{\text{cond}, 1-3} + b_0 T_{\text{os}, 1-0} + b_1 T_{\text{os}, 1-1} + b_2 T_{\text{os}, 1-2} + b_3 T_{\text{os}, 1-3} - T_i \sum c_n$$

After substituting the known values into the above equation gives

$$Q_{\text{cond}, 1} = -(-0.94420)(0.00) - 0.05025(0.00) - (-0.00008)(0.00) + 0.00312(24.4) \\ + 0.04173(25.0) + 0.02736(26.1) + 0.00119(27.2) - 2.0(0.0734)$$

$$Q_{\text{cond}, 1} = 0.03 \text{ W/m}^2.$$

The above process of calculation for  $Q_{\text{cond}, 1}$  is repeated for four or five days, the value appears to be stabilized by the fourth day.

It may be noted that the conductive heat gain reaches maximum at  $t = 19.00 \text{ hrs}$ , which is 3 hours after the peak of the sol-air temperature indicating the effect of thermal storage.

**Table 3 Iterative Process of Transfer Function Method in Calculation of Heat Gain through a Wall**

T	$T_{os,t}$	$Q_{cond,t}$	$Q_{cond,t+24}$	$Q_{cond,t+48}$	$Q_{cond,t+72}$
Hr	$^{\circ}\text{C}$	$\text{W/m}^2$	$\text{W/m}^2$	$\text{W/m}^2$	$\text{W/m}^2$
-2	27.2	0.00			
-1	26.1	0.00			
0	25.0	0.00			
1	24.4	0.03	9.29	9.82	9.85
2	24.4	0.00	8.22	8.69	8.72
3	23.8	-0.04	7.25	7.67	7.70
4	23.3	-0.11	6.36	6.73	6.76
5	23.3	-0.21	5.53	5.86	5.88
6	25.0	-0.32	4.79	5.08	5.10
7	27.7	-0.33	4.2	4.46	4.48
8	30.0	-0.17	3.85	4.08	4.10
9	32.7	0.16	3.74	3.94	3.95
10	35.0	0.66	3.83	4.01	4.02
11	37.7	1.29	4.10	4.26	4.27
12	40.0	2.04	4.54	4.68	4.69
13	53.3	2.94	5.15	5.28	5.29
14	64.4	4.40	6.37	6.48	6.49
15	72.7	6.59	8.34	8.44	8.44
16	75.5	9.26	10.81	10.9	10.91
17	72.2	12.02	13.4	13.48	13.48
18	58.8	14.4	15.62	15.69	15.69
19	30.5	15.77	16.86	16.92	16.92
20	29.4	15.39	16.36	16.41	16.41
21	28.3	14.13	14.98	15.03	15.03
22	27.2	12.84	13.60	13.64	13.64
23	26.1	11.60	12.28	12.32	12.32
24	25.0	10.42	11.02	11.05	11.06

### Key Parameters Related to Wind Turbines:

Following definitions are obtained from reference [19].

Undisturbed Wind Velocity,  $V$ : The wind velocity just before striking the wind blades.

Blade Velocity,  $V_b$ : It is the tangential velocity ( $U$ ) of the tip of the turbine blade.

The Speed Ratio,  $\lambda$ : It is the ratio of the blade velocity ( $V_b$ ) to the undisturbed Wind Velocity ( $V$ ) of the wind,  $\lambda = V_b/V$ .

Pitch angle or angle of attack,  $\beta$ : It is the angle made by the relative velocity of the wind with the chord angle of the blade or it is the angle made by the plane of the blade with its longitudinal axis. See Figure 1 below.

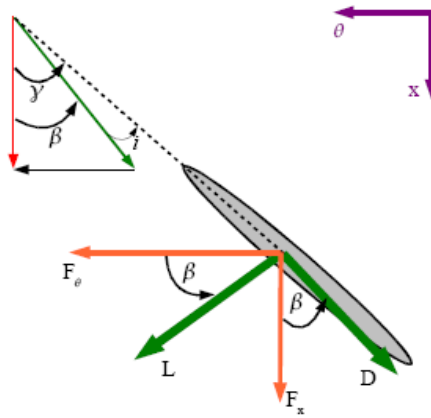


**Figure 1** Angle and forces on the blade of wind turbine [20]

Lift,  $L$ : It is the force experienced by an object immersed in a flowing fluid in the direction normal to the direction of the fluid flow given by  $0.5 C_L \rho A V^2$ . The upward lift force is created by two ways; one is by the wind flowing over the top of the blade

creating pulling pressure (negative pressure), second is by the air flowing below the blade creating pushing pressure (positive pressure). See Figure 3.2(b).

Drag, D: It is the force experienced by an object immersed in a flowing fluid in the direction parallel to the direction of the fluid flow given by  $0.5 C_D \rho A V^2$ .

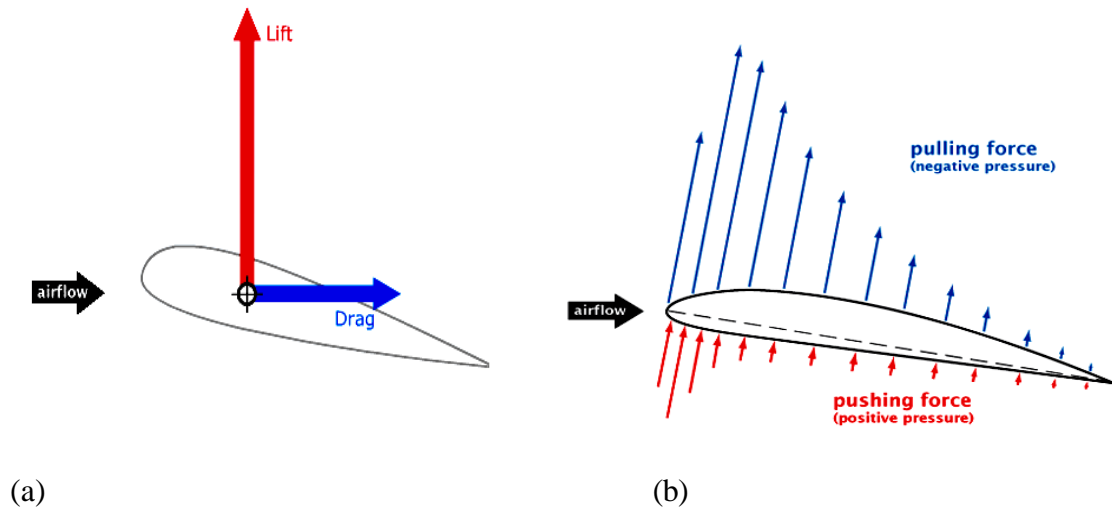


**Figure 2** Lift and Drag Forces on the wind turbine blade [20]

Swept Area, A: It is the area swept by the wind turbine blades, when exposed to atmosphere and wind.

Coefficient of Lift Force,  $C_L$ : It is the ratio of the lift force to the internal force and is given by  $C_L = L / (0.5 \rho A V^2)$

Coefficient of Drag Force, D: It is the ratio of the drag force to the internal force and is given by  $C_D = D / (0.5 \rho A V^2)$

Coefficient of Power,  $C_P$ : It is the ratio of the power produced by the wind turbine to the maximum power that can be produced and is given by  $C_P = P / P_{\max}$

Cut-in Wind Speed: It is the minimum speed of the wind that has potential to produce some wind power by rotating the wind turbine blades.

Shut-down Wind Speed: It is the maximum speed of the wind that can damage the wind turbine blades, rotor and other structural damage.